EUROPEAN COMMISSION
Community Research

SEVENTH FRAMEWORK PROGRAMME

CARBOWASTE

Treatment and Disposal of Irradiated Graphite and Other Carbonaceous Waste

Grant Agreement Number: FP7-211333

Technical Report T-3.4.3
Modelling of isotope release mechanism based on fission product transport codes

Author(s):
Ernestas Narkunas, Povilas Poskas; LEI
Greg Black, Abby Jones; UoM
Constantin Iorgulis, Daniela Diaconu; INR
Laurent Petit, Bernard Poncet; EDF

Date of issue of this report: 15/02/2013

Project co-funded by the European Commission under the Seventh Framework Programme (2007 to 2011) of the European Atomic Energy Community (EURATOM) for nuclear research and training activities		
Dissemination Level		
PU	Public	
RE	Restricted to the partners of the CARBOWASTE project	**X**
CO	Confidential, only for specific distribution list defined on this document	

Start date of project: **01/04/2008** Duration: **60 Months**

Distribution list

Person and organisation name and/or group	Comments
Werner von Lensa, FZJ	
Gabriel Pina, CIEMAT	
Abbie Jones, UoM	
Daniela Diaconu, INR	
Laurent Petit, EDF	

CARBOWASTE		
Work package: 3 **Task:** 3.4	**CARBOWASTE document no.:** CARBOWASTE-1302-T-3.4.3 (e.g. May 2008 as date of issue: 0805)	**Document type:** T=Technical Report
Issued by: LEI (LT) **Internal no.:** CW1302-Deliverable-T-3-4-3-final		**Document status:** Final

Document title

Modelling of isotope release mechanism based on fission product transport codes

Executive summary

The Work Package 3 (Characterisation and Modelling) Task 3.4 (Modelling the Behaviour of Impurities and Isotopes in Graphite) focuses on modelling of the changes in graphite radiological inventory (list of present radionuclides and their activity) during reactor operation and after its final shutdown.
This report presents results of the main radionuclides formation mechanisms in the reactor graphite under neutron irradiation and possible their release mechanisms. The presented results are for MAGNOX, UNGG, RBMK and TRIGA reactors from UK, France, Lithuania and Romania. The modelling results are compared with the available measurement data and observed differences are described identifying main processes influencing those differences.

Revisions

Rev.	Date	Short description	Author	Internal Review	Task Leader	WP Leader
00	dd/mm/yyyy	Issue	Name, Organisation *Signature*	Name, Organisation *Signature*	Name, Organisation *Signature*	Name, Organisation *Signature*
01	27/04/2012	First issue	Narkunas LEI	Poskas LEI	Jones UoM	Pina CIEMAT
02	17/09/2012	Second issue	Narkunas LEI	Poskas LEI	Jones UoM	Pina CIEMAT
03	15/02/2013	Final issue	Narkunas LEI	Poskas LEI	Jones UoM	Pina CIEMAT

Table of Content

Figures

Tables

1 Introduction

Ignalina NPP, located in *Lithuania*, has two Units with RBMK-1500 water-cooled graphite-moderated channel-type power reactors. One of the most important radionuclides in the activated RBMK reactors graphite is a long-lived ^{14}C. The propagation of cooling helium-nitrogen gases mixture (which circulates around RBMK reactor graphite stack) into the graphite pores may additionally increase the quantity of nitrogen impurity and consequently increase ^{14}C production in RBMK-1500 reactor's graphite blocks and rings/sleeves. So a conservative estimation of possible nitrogen impurity content coming from the cooling gases of RBMK-1500 reactor graphite stack was also made, and as a result an axial distribution of induced ^{14}C activity in the RBMK-1500 reactor's graphite blocks and rings was achieved. Calibration of developed models against experimental activity measurement data of irradiated graphite ring specimen from RBMK-1500 reactor was performed too. It was done by the reverse activation modelling way, i.e. the concentrations of impurities, which activation lead to the generation of particular radionuclide, were altered until the modelled activity of that radionuclide matches best the measured one. It was observed, that using "explanatory" impurities concentrations, which were derived in reverse activation modelling way, modelled specific activities of most of measured radionuclides (^{14}C, ^{54}Mn, ^{60}Co, ^{134}Cs, ^{137}Cs, ^{154}Eu, ^{155}Eu, ^{238}Pu, $^{239+240}Pu$, ^{241}Am and $^{243+244}Cm$) were in rather good agreement with the measurement results (with exception of ^{152}Eu and ^{242}Cm radionuclides).

When all operational reactors are shutdown the *United Kingdom* will have a graphite waste legacy of 99000 tonnes, this waste contains a variety of radionuclides and will fall under the Intermediate Level Waste classification, for which the UK does not have a current disposal policy. Characterisation of the end of life radionuclide inventory is required before any policy can be developed, a combined programme of experimental and simulated work has been undertaken to investigate this. The ^{3}H, ^{14}C and ^{60}Co content of a trepanned sample from Wylfa MAGNOX Reactor 1 have been experimentally determined using beta liquid scintillation counting and gamma spectroscopy. The WIMS9A reactor code and FISPACT-2007 neutron activation software have also been used to calculate this samples' inventory, considering only a model which is isolated from the reactor circuit. Comparison between experimental and calculated results has shown that the original impurity levels are sufficient to explain the end of

life activity, without additional consideration of contamination from other materials in the reactor circuit, in this type of simulation. Additionally the calculations show that the production of ^{14}C from ^{14}N is approximately equal to that produced from ^{13}C.

In *Romania*, the TRIGA Materials Test Reactor is situated at INR, Pitesti. The thermal column of TRIGA reactor consists of 96 rectangular bricks of graphite encased in Aluminium, arranged in 12 rows of 8 bricks. The graphite used in TRIGA thermal column is sintered graphite produced in UK in the '50 with a density of 1.72 g/cm^3. The total weight of graphite brick is 24.97 kg and the whole column weights 2.447 t. The modelling tools used for the assessment of the radionuclide content in the graphite irradiated in the thermal column of TRIGA reactor were: WIMS for cross section generation, DFA for flux and power distribution and ORIGEN-S for nuclide activities evaluation. Several modelling cases were developed and radioactivity of graphite for these cases was evaluated. The modelled results (assuming initial impurities in graphite) show general good agreement with the measured activities of ^{3}H ^{14}C ^{60}Co ^{152}Eu and ^{154}Eu radionuclides.

EDF was in *France* the operator of six gas-cooled reactors, all shutdown now. They will have to be dismantled as soon as possible, and at least by 2022 for the retrieval of the first graphite brick from the Bugey 1 reactor. These reactors are of so-called in French, "UNGG" reactor type. They were graphite moderated, cooled by carbon dioxide and fuelled with natural uranium. Concerning graphite in UNGG reactors, this material was used in different parts of the reactors as a moderating element in the core, as mechanical support of the fuel cartridge in the fuel channels of the pile (graphite sleeves) and also as a biological shield under the pile in the case of the so-called integrated vessel reactors. The total amount of irradiated graphite for EDF UNGG reactors is about 17 000 t. It consists of 13 000 t of graphite bricks from the piles of the six UNGG reactors, 2 000 t of graphite sleeves in silos in Saint-Laurent and 2 000 t of graphite used as biological shield under the core of integrated vessel type reactors – Saint-Laurent A1 & A2, Bugey 1. The radioactivity of the graphite in UNGG comes almost exclusively from the activation under neutron flux of the impurities and carbon present in the material. With the production of radionuclides by activation, it is also necessary, out of a principle of exhaustiveness, to take into account a certain number of other phenomena which may also have had an influence on the radiological inventory of the graphite during the operation of the reactor.

2 Lithuania

Ignalina NPP (INPP) in the only one NPP in Lithuania, which consists of two Units with RBMK-1500 water-cooled graphite-moderated channel-type power reactors. Unit 1 was shut down at the end of 2004 while Unit 2 was shut down in the end of 2009 and Ignalina NPP is under the decommissioning stage now.

Cross section of RBMK-1500 reactor vault is presented in Fig. 1 [1].

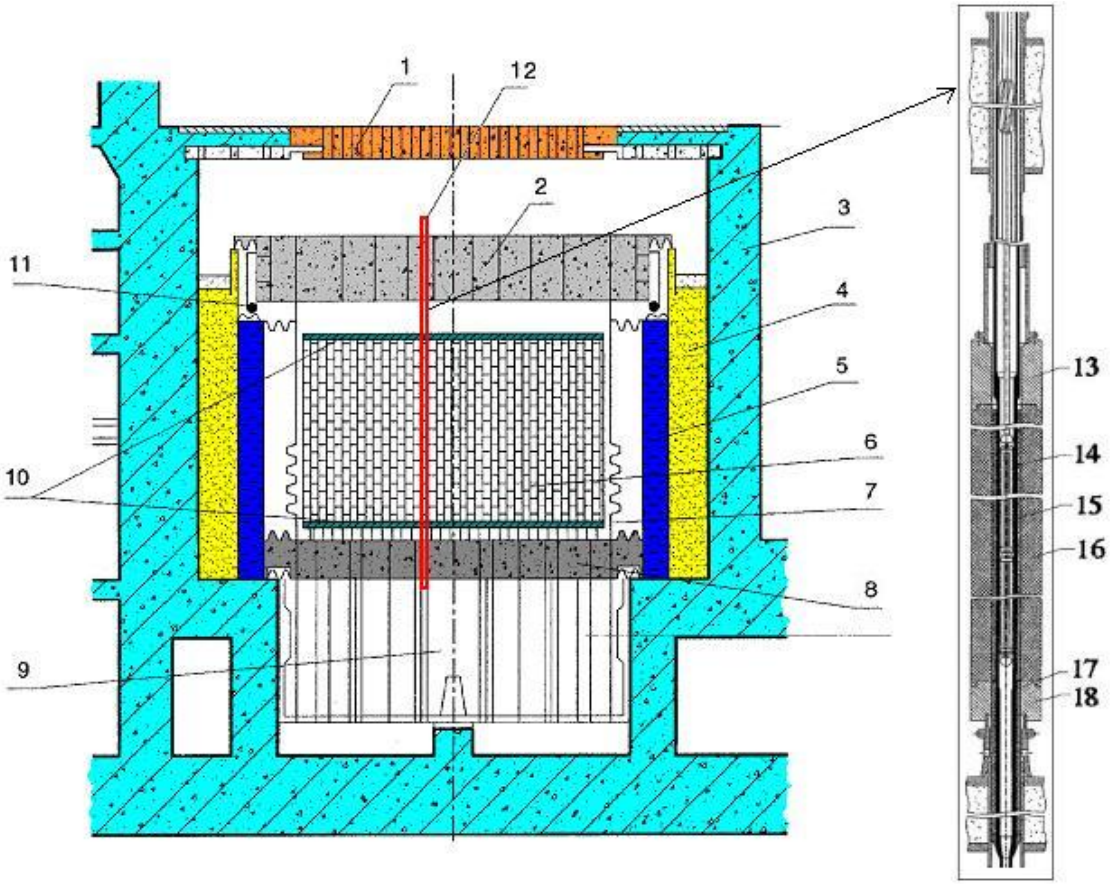

Fig. 1. Cross–section of RBMK–1500 reactor vault [1]

1 – top cover (floor of the central hall);
2 – top metal structure (with serpentinite);
3 – concrete vault;
4 – sand cylinder;
5 – water tank;
6 – graphite stack;
7 – reactor shell;
8 – bottom metal structure (with serpentinite);
9 – reactor support structure;
10 – steel shield and support plates;
11 – roller supports;
12 – modelled segment;
13 – shield plate;
14 – FC central part;
15 – FA inside FC;
16 – graphite blocks;
17 – graphite rings/sleeves;
18 – support plate

The graphite stack (6) serves as a neutron moderator and reflector. The graphite stack (8 m height and 14 m in diameter) consists of individual graphite blocks (16) made of GR-280 grade

graphite, stacked into the 8 m height 2488 columns. The blocks are rectangular parallelepipeds, with a base of 0.25 × 0.25 m, and heights of 0.2, 0.3, 0.5 and 0.6 m, having vertical bore openings used for positioning of the channels, which in turn are used for placing fuel assemblies, control rods and several types of instruments into the core. The upper and the lower 0.5 m thick graphite stack layers are called respectively top and bottom reflectors while the outer peripheral 444 graphite columns (forming ~1 m thick outer ring) serve as radial reflector. The channel is located in the central hole of the brick and its central segment is surrounded by a system of 0.02 m high and 0.0115 m thick split GRP-2-125 grade graphite rings (17). Each ring is alternately tight on the pressure tube or tight in the bore of the brick. The slots in the graphite rings are aligned to allow the gas mixture to pass along the channel. Above and below graphite rings there are also placed GRP-2-125 grade graphite sleeves of different shape compared to the rings. To prevent oxidation of the graphite and to improve the thermal efficiency, the core is filled with a circulating helium-nitrogen mixture.

2.1 Assessment of possible ^{14}C production ways in RBMK-1500 reactor's irradiated graphite

One of the most important radionuclides in the activated RBMK reactors graphite is a long-lived ^{14}C [2, 3]. The fraction of produced ^{14}C from the raw carbon activation may be calculated quite precisely as the quantity of carbon in graphite is almost invariant and comprises more than 99.9 % of mass, while the fraction coming from impurities (nitrogen and oxygen) activation differs depending on these impurities initial content, as presented in CARBOWASTE project Technical Report T-3.4.2 [4]. Furthermore, the propagation of cooling helium-nitrogen gas mixture in the graphite pores may additionally increase the quantity of nitrogen impurity and consequently increase ^{14}C production and this § 2.1 chapter namely presents modelling results of nitrogen impurity impact to the ^{14}C production in Ignalina NPP Unit 1 RBMK-1500 reactor's graphite blocks and rings/sleeves.

2.1.1 Methodology and assumptions

In this § 2.1 chapter, axial distributions of ^{14}C specific activity in the reactor RBMK-1500 graphite structures (blocks and rings/sleeves) at reactor final shutdown (RFS) from the results presented in Technical Report T-3.4.2 [4] are obtained, and the points of maximal ^{14}C specific activity (in axial reactor direction) are identified. Then the influence of nitrogen impurity

content on produced ^{14}C specific activity in the graphite blocks and rings/sleeves is analysed at the points where the highest ^{14}C specific activities are observed.

Minimal and maximal concentrations of all possible impurities for RBMK-1500 reactors' graphite blocks and graphite rings/sleeves were used when obtaining axial ^{14}C activities distributions, as presented [4]. Then for modelling of nitrogen impurity influence on ^{14}C production in the graphite blocks and rings/sleeves (at the points where the highest ^{14}C activity in the axial direction is observed) several new modelling cases were developed.

No impurities were taken into account (also initial nitrogen content was chosen to be 0 % of mass), i.e. pure graphite was assumed for the first newly developed modelling case. After that for other developed subsequent modelling cases different initial nitrogen impurity content in the graphite – up to 0.05 % of mass (no other impurities) was assumed. All other modelling parameters and assumptions for these cases were generally the same as presented in [4].

2.1.2 Results and discussion

Modelled ^{14}C activity distribution in the graphite blocks and rings/sleeves (using already modelled neutron fluxes, see [4]) along the reactor axis after the RFS is presented in Fig. 2.

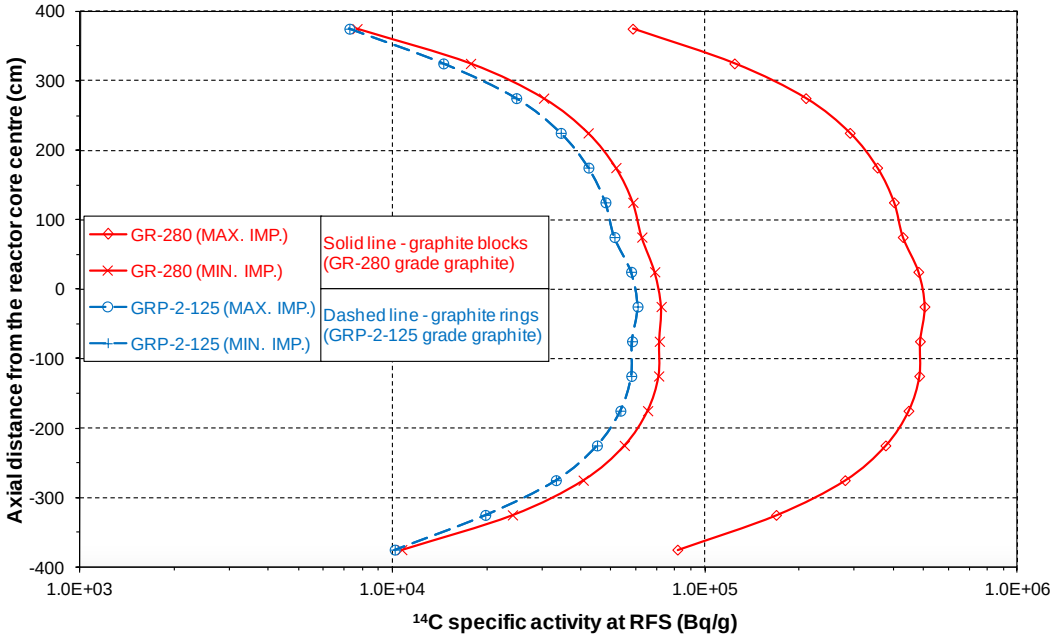

Fig. 2. ^{14}C activity distribution along reactor axis in graphite structures

MAX. IMP. – ^{14}C activity obtained using maximal concentrations of all impurities from published sources;
MIN. IMP. – ^{14}C activity obtained using minimal concentrations of all impurities from published sources

^{14}C activity distribution is almost identical in the graphite rings/sleeves for minimal and maximal initial impurities concentrations (Case A and Case B, see [4]). This is because there is no data on nitrogen and oxygen impurities in GRP-2-125 grade graphite in published sources (see Technical Report T-3.4.2 [4]), thus these impurities were not taken into account in modelling and all produced ^{14}C for the graphite rings/sleeves comes practically only from activation of carbon in both cases. However, it should be noted, that absence of nitrogen or oxygen impurities data for GRP-2-125 grade graphite does not mean that there are no these impurities. Usually methods used for qualitative and quantitative impurities determination, as stated in [5], are not suitable for nitrogen and other light elements and thus no data for these elements are provided.

For graphite blocks situation is different. For maximal initial impurities concentrations case (Case A, see [4]) ^{14}C activity is about 7 times higher than for minimal concentrations case (Case B, see [4]). This difference is influenced mostly by nitrogen impurities in GR-280 grade graphite, because initial nitrogen concentration was $4 \cdot 10^{-5}$ % of mass [6] for minimal concentration case while for maximal concentrations case it was $7 \cdot 10^{-3}$ % of mass [7], see [4]. Oxygen concentration was $1.8 \cdot 10^{-4}$ % of mass [6] for both modelling cases.

The modelling results also show that ^{14}C activity distribution along the axial direction in the graphite rings/sleeves and blocks corresponds to the thermal neutron flux distribution (see Technical Report T-3.4.2 [4] and Fig. 2) for all modelled cases. Maximal ^{14}C activity position coincides with the maximal thermal neutron flux position and (analogous to thermal flux) ^{14}C activity in the top and bottom parts is respectively ~8 and ~6 times lower than the maximal activity. This confirms the fact that production of ^{14}C from carbon activation, as well as from impurities activation, is determined mainly by thermal neutron flux.

The average ^{14}C activity in the active core graphite blocks (i.e. average in the 700 cm height central part of graphite blocks column) for the minimal and maximal impurities cases are ~$5.2 \cdot 10^4$ and ~$3.6 \cdot 10^5$ Bq/g respectively. These results are generally in good agreement with earlier presented results of preliminary INPP GR-280 graphite activation modelling (obtained ^{14}C specific activity is ~$4.2 \cdot 10^4$ and ~$3.4 \cdot 10^5$ Bq/g respectively for the minimal and maximal impurities cases) [8], where activation modelling was performed assuming constant neutron flux and 20 years of continuous plant operation. Results of another estimation [5] shows

slightly higher – ~5.0·10^5 Bq/g average activity of ^{14}C in graphite moderator. However, in neither of these estimations ([5, 8]) any assumptions on possible quantity of nitrogen absorbed from the reactor cooling gases in graphite pores have been made.

The position of maximal ^{14}C activity, as already mention above, coincides with the maximal thermal neutron flux position and is situated at ~25 cm below the axial rector centre (elevation mark -25 cm in the Fig. 2). For this point, i.e. using modelled neutron fluxes in this position, the influence of nitrogen impurity content on produced ^{14}C activity in the graphite blocks and rings/sleeves was analysed. This radionuclide, as mentioned earlier, in nuclear reactors graphite may be produced mainly in two different ways: from activation of raw graphite material – carbon and from activation of impurities (nitrogen and oxygen) via five main reactions [9]: 1) $^{13}C(n,\gamma)^{14}C$; 2) $^{14}N(n,p)^{14}C$; 3) $^{17}O(n,\alpha)^{14}C$; 4) $^{15}N(n,d)^{14}C$; 5) $^{16}O(n,^3He)^{14}C$.

The production of ^{14}C from the last two (4th and 5th) reactions is not the case for thermal neutron reactors (for example RBMK) as these reactions are highly endothermic ($Q \approx -8$ MeV for 4th and $Q \approx -15$ MeV for 5th reaction) and requires higher neutron energies [9, 10] which are reached in fast neutrons or in fusion reactors. Thus main possible ^{14}C production reactions in RBMK reactor's graphite are presented in Table 1.

Table 1. Main possible ^{14}C production reactions in RBMK reactor's graphite [2, 3]

Isotope of chemical element	Reaction	Cross-section for thermal neutrons (barns)	Abundance of isotope in naturally occurring chemical element (%)
^{13}C	$^{13}C(n,\gamma)^{14}C$	0.0009	1.07 in natural C
^{14}N	$^{14}N(n,p)^{14}C$	1.8	99.63 in natural N
^{17}O	$^{17}O(n,\alpha)^{14}C$	0.235	0.04 in natural O

Due to the small $^{17}O(n,\alpha)^{14}C$ reaction cross-section and very low abundance of ^{17}O isotope in natural oxygen, production of ^{14}C from this reaction is ~2·10^4 times lower than production from $^{14}N(n,p)^{14}C$ reaction for the same initial quantity of naturally occurring oxygen and nitrogen impurities (see Table 1). Combining this and the fact, that reported quantities of initial oxygen and nitrogen impurities in GR-280 grade graphite are somewhat in the comparable order of magnitude (oxygen – 1.8·10^{-4} % of mass, nitrogen – (0.4–70)·10^{-4} % of mass, see [4]), allows to consider $^{17}O(n,\alpha)^{14}C$ reaction as insignificant source of ^{14}C production. Furthermore, the absence of oxygen in RBMK reactor cooling gas (maximal allowed volumetric concentration of oxygen in cooling gas during reactor operation is only 0.005 %, whereas

nitrogen concentration is in the range of 5–100 % [11, 12]) also sustains statement above and due to that oxygen impurity influence to ^{14}C production was neglected in the analysis.

Results of performed analysis of nitrogen impurity content influence on produced ^{14}C in RBMK-1500 reactor's graphite are presented in Fig. 3. It shows total ^{14}C activity dependence on initial nitrogen impurity content in the graphite blocks and rings/sleeves, as well as different ways of ^{14}C production from carbon (raw material of graphite) and nitrogen (impurity). The production of ^{14}C from carbon stays practically constant changing the nitrogen content in analysed 0–0.05 % mass range, because the mass of main chemical element (carbon) in graphite practically stays unchanged (100–99.95 % of mass). Activity of ^{14}C produced from carbon activation in this case comprises ~$6.1 \cdot 10^4$ Bq/g in the graphite rings/sleeves and ~$7.0 \cdot 10^4$ Bq/g in the graphite blocks. This difference of activities is directly related to the thermal neutron flux differences in graphite blocks and rings/sleeves, i.e. ~1.2 time higher activity in graphite blocks is due to the ~1.2 time higher thermal neutron flux in graphite blocks, compared to those in rings/sleeves, see Technical Report T-3.4.2 [4].

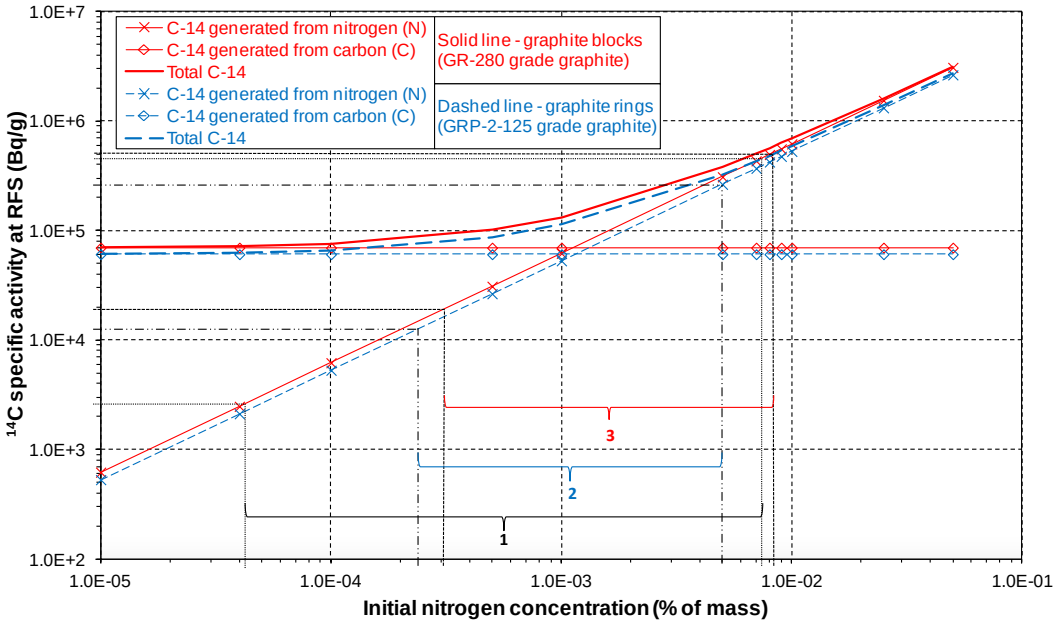

Fig. 3. ^{14}C activity dependence on initial nitrogen impurity concentration

interval 1 – nitrogen concentration in GR-280 grade graphite matrix from published sources;
interval 2 – calculated nitrogen concentration in GRP-2-125 grade graphite pores;
interval 3 – calculated nitrogen concentration in GR-280 grade graphite pores

The production of ^{14}C from nitrogen activation increases linear while increasing nitrogen content, and at ~$1.1 \cdot 10^{-3}$ % nitrogen mass concentration equals ^{14}C production from carbon activation. The activity of ^{14}C produced from nitrogen activation (at the same initial concentration) in the graphite blocks is also ~1.2 time higher than in the graphite rings/sleeves due to the mentioned differences of thermal neutron fluxes.

Modelling results show (Fig. 3) that for nitrogen impurity concentrations up to $1 \cdot 10^{-4}$ % mass, the activity of ^{14}C produced from nitrogen impurity activation is considerably lower than that of carbon activation and does not influences total ^{14}C activity. However, when nitrogen impurity concentration reaches ~$1.1 \cdot 10^{-3}$ % mass, the production of ^{14}C from nitrogen activation equals the production from carbon activation and with further increase of nitrogen concentration $^{14}N(n,p)^{14}C$ reaction becomes dominant.

So, for nitrogen impurity concentrations from $4.0 \cdot 10^{-5}$ to $7.0 \cdot 10^{-3}$ % mass (marked as interval "1" in Fig. 3) in GR-280 grade graphite (see Technical Report T-3.4.2 [4]), the total activity of ^{14}C varies from ~$7.0 \cdot 10^{4}$ to ~$5.0 \cdot 10^{5}$ Bq/g where ^{14}C produced from carbon activation always comprises ~$7.0 \cdot 10^{4}$ Bq/g. There is no data on initial nitrogen impurity in GRP-2-125 grade graphite (see Technical Report T-3.4.2 [4]), however assuming that there can be the same nitrogen impurity concentration as in GR-280 grade graphite, the activity of total produced ^{14}C would be about 1.2 time lower than of GR-280 grade graphite and ^{14}C produced from carbon activation would comprise ~$6.0 \cdot 10^{4}$ Bq/g.

Published data on initial nitrogen impurities in graphite are for virgin graphite and may be conservatively considered as impurities incorporated into the graphite matrix. However, graphite is a porous material and porosity of GR-280 grade graphite is about 23 % (17 % are for open and 6 % are for closed pores volume) [13], while porosity of GRP-2-125 grade graphite is about 16 % (14 % are for open and 2 % are for closed pores volume) [14]. As RBMK reactors' graphite stack is cooled with mixture of helium-nitrogen gases, nitrogen can penetrate into the open graphite pores and additionally increase its concentration in the graphite. Depending on reactor operation state nitrogen volumetric content in the gases may be in the range of 5–100 % and there are 3 basic cooling gases volumetric compositions [11, 12]:

- Dry air (where N_2 comprises about 80 %). This is for an auxiliary regime which is only used for a shutdown reactor;

- Nitrogen (100 % N_2). This is for an auxiliary regime which is used at the reactor power below 750 MW(e);
- Helium-nitrogen mixture (90 % He + 10 % N_2). This is for normal reactor power operation.

Taking into account the facts that cooling gases circulates in the rector sealed space at an excess pressure of 0.49–1.96 kPa and that gas temperature is about 350 ^{o}C, the concentration of N_2 gas (number of N_2 molecules) in 1 cm^3 volume of 100 % N_2 gas cooling mode may be calculated using the ideal gas law (pV=nkT):

$$n = \frac{pV}{kT}; \quad (1)$$

where

n – number of N_2 gas molecules;
p – pressure in Pa (N/m^2);
V – volume in m^3 (for 1 cm^3 in this case it is $1 \cdot 10^{-6}$ m^3);
k – Boltzmann's constant;
T – gas temperature in K.

For an excess pressure of 0.49 kPa equation (1) gives $1.18 \cdot 10^{19}$, while for an excess pressure of 1.96 kPa – $1.20 \cdot 10^{19}$ N_2 molecules/cm^3. This shows that N_2 gas concentration in cooling gases varies insignificantly depending on operational pressure, however taking into account possible cooling gas volumetric composition (5–100 % of N_2 gases) and pressure, the concentration of N_2 gas may vary in the range of $5.92 \cdot 10^{17}$ to $1.20 \cdot 10^{19}$ N_2 molecules/cm^3.

Knowing this and N_2 molecular weight it is possible to calculate the quantity of N_2 gases which additionally may increase the nitrogen impurity content in the graphite. Assuming that cooling gases penetrate into the graphite structures and fill all open pores during reactor operation, for GR-280 grade graphite (having 1.65 g/cm^3 density and 17 % open porosity) this quantity is in the range of $2.8 \cdot 10^{-4}$ to $5.8 \cdot 10^{-3}$ %, while for GRP-2-125 grade graphite (having 1.85 g/cm^3 density and 14 % open porosity) it is in the range of $2.1 \cdot 10^{-4}$ to $4.2 \cdot 10^{-3}$ % of initial graphite mass for any possible cooling gas pressure and volumetric composition. Furthermore, assuming that cooling gases in the graphite may fill not only open but closed pores also,

nitrogen impurities from cooling gases then may be in the range of $3.8 \cdot 10^{-4}$ to $7.8 \cdot 10^{-3}$ % for GR-280 grade graphite, and in the range of $2.3 \cdot 10^{-4}$ to $4.6 \cdot 10^{-3}$ % of initial GRP-2-125 grade graphite mass.

Generally, the cooling gases cannot easy penetrate into the closed graphite pores, thus assumption that these gases fill all pores volume seems unlike together with the fact, that e.g. the porosity of virgin (unirradiated) and of irradiated GRP-2-125 grade graphite is practically the same having the same proportions for open and closed pores volumes [14]. However, the dynamic of closed and open pores in the graphite under irradiation is not well known (do the pores stays as are or do the closed pores became open while open pores evolve into the closed, and etc.) and the possibility that closed pores in graphite may contain air (nitrogen comprises ~80 % of vol.) trapped in these pores during graphite manufacture processes, the assumption that all pores may contain nitrogen gas is still relevant.

Table 2 gives minimal and maximal calculated nitrogen concentrations in GR-280 and GRP-2-125 grades graphite (due to the cooling gas penetration into the graphite pores) for any possible cooling gas composition and operating pressure.

Table 2. Possible calculated nitrogen concentrations in GR-280 and GRP-2-125 grades graphite due to the cooling gas penetration into the graphite pores

Cooling gas excess pressure, kPa	**0.49**	**1.96**
Nitrogen volumetric fraction in cooling gas, %	**5**	**100**
Assuming, that cooling gas fills only open pores in graphite		
Nitrogen concentration in GR-280 graphite, % from initial graphite mass	$2.8 \cdot 10^{-4}$	$5.8 \cdot 10^{-3}$
Nitrogen concentration in GRP-2-125 graphite, % from initial graphite mass	$2.1 \cdot 10^{-4}$	$4.2 \cdot 10^{-3}$
Assuming, that cooling gas fills all (open and closed) pores in graphite		
Nitrogen concentration in GR-280 graphite, % from initial graphite mass	$3.8 \cdot 10^{-4}$	$7.8 \cdot 10^{-3}$
Nitrogen concentration in GRP-2-125 graphite, % from initial graphite mass	$2.3 \cdot 10^{-4}$	$4.6 \cdot 10^{-3}$

The ranges for possible calculated nitrogen concentrations in GRP-2-125 and GR-280 grades graphite due to cooling gas absorption in all pores are marked respectively as interval “2” and “3” in Fig. 3. The range of initial nitrogen impurity concentration in GR-280 graphite matrix from published sources is marked as interval “1”.

So, for the very conservative case, assuming maximal initial nitrogen concentration in the GR-280 grade graphite matrix ($7.0 \cdot 10^{-3}$ %) and maximal initial nitrogen concentration from cooling gases in the graphite pores ($7.8 \cdot 10^{-3}$ %), total ^{14}C activity in this graphite at the point of maximal thermal neutron flux is about $9.9 \cdot 10^{5}$ Bq/g, where ^{14}C produced from carbon activation comprise only ~7 %, while remaining 44 % and 49 % are for ^{14}C produced from nitrogen impurity in the graphite matrix and nitrogen gas in the graphite pores respectively. Similarly, assuming the same initial maximal nitrogen impurity concentration for GRP-2-125 grade graphite (the same as for GR-280) and maximal initial nitrogen concentration from cooling gases in the graphite pores ($4.6 \cdot 10^{-3}$ %), total ^{14}C activity in this graphite at the point of maximal thermal neutron flux is about $6.8 \cdot 10^{5}$ Bq/g, where ^{14}C produced from carbon activation comprise ~9 %, while remaining 55 % and 36 % are for ^{14}C produced respectively from nitrogen impurity in the graphite matrix and nitrogen gas in the graphite pores. However, it should be emphasised that above estimated activity of ^{14}C in the graphite pores is based on a conservative assumption that all produced ^{14}C remains in the pores (not escaping into the cooling gases).

The analysis also showed that even at the point of maximal thermal neutron flux, the burn up of initial nitrogen impurity is not significant, i.e. the remaining nitrogen impurity mass after 21 year Ignalina NPP Unit 1 reactor operation is still 96 % of the initial. Thus for modelling purposes, the fact that during reactor operation cooling gases circulates around the graphite structures and nitrogen concentration in the graphite pores may always be the same as initial, may be ignored, i.e. it is enough to define only initial nitrogen impurity content.

^{14}C activity dependence on initial nitrogen impurity concentration at the point of maximal thermal neutron flux (see Technical Report T-3.4.2 [4]), may be expressed using simple equations (2) and (3) respectively for the graphite blocks and rings/sleeves at RFS:

$$A_{^{14}C} \approx 6.2 \times 10^{7} \times C_N + 7.0 \times 10^{4}; \quad (2)$$

$$A_{^{14}C} \approx 5.3 \times 10^{7} \times C_N + 6.1 \times 10^{4}; \quad (3)$$

where

$A_{^{14}C}$ – specific activity of ^{14}C in Bq/g;

C_N – initial concentration of nitrogen impurity in graphite in % of mass.

The equations (2) and (3) are valid only at the points of maximal thermal neutron fluxes and for nitrogen concentrations up to ~0.1 % of mass, i.e. while carbon concentration in graphite may be considered as constant.

Similar equations are presented for Bugey-1 reactor graphite sleeves [15], giving that ^{14}C activity may be also calculated using simple linear equations expressing ^{14}C production from carbon, nitrogen and oxygen activation. These evaluations for Bugey-1 graphite sleeves are in good agreement with the ones for ^{14}C production in RBMK reactor, showing that ^{14}C production from oxygen is $\sim 2.0 \cdot 10^{4}$ times lower than production from the same quantity of nitrogen and that production of ^{14}C from nitrogen equals ^{14}C production from carbon when nitrogen impurity content is 10–11 ppm ($(1–1.1) \cdot 10^{-3}$ %) [15].

From the point of view of irradiated graphite ^{14}C nuclide decontamination, analysis results may also be interpret in the way, that there can be four major fractions of ^{14}C release/removal from irradiated RBMK reactors graphite.

The first, and likely the most difficult to remove is the fraction of ^{14}C coming from ^{13}C activation in graphite matrix, which can be in the order of 10^{4} Bq/g for both graphite grades.

The second fraction is associated with activation of nitrogen impurities, which are incorporated in the virgin graphite matrix. This fraction of ^{14}C looks like also difficult to remove from irradiated graphite and may be in the order up to 10^{5} Bq/g depending on initial nitrogen impurity concentration.

The third and fourth fractions are related to the nitrogen adsorption/penetration from cooling gases into the graphite pores and its activation. The fraction of ^{14}C being produced in the open pores may be in the order of 10^{5} Bq/g in the most conservative case and in the closed pores it may be about 3 times lower for GR-280 grade graphite and about 7 times lower for GRP-2-125 grade graphite. These fractions of ^{14}C looks like the easiest fractions to remove (the fraction from open pores being more easy) during graphite decontamination, as produced ^{14}C is probably only adsorbed on the surfaces of the graphite pores and as free gases inside them, without being incorporated into the graphite matrix.

Several examples of experimental and numerical estimations of the radioactive inventories in various irradiated graphites are gathered and presented in ref. [3] appendix F. Results provided

for ^{14}C activity show, that in general ^{14}C activity is in the range of $(1–10)\cdot10^4$ Bq/g, but depending on graphite and reactor type, location, operation history and etc., the lowest ^{14}C activity may be in the order of 10^3 Bq/g, while the highest – in the order of 10^6 Bq/g. This indicates general compliance with the results presented here for Ignalina NPP RBMK-1500 reactor (see Fig. 2, Fig. 3 and Table 3).

Table 3. Summarised data of ^{14}C activities in graphite

Assumption (or reference)	**Min. ^{14}C activity, Bq/g**	**Max. ^{14}C activity, Bq/g**	**Avg. ^{14}C activity, Bq/g**
Modelling of Ignalina NPP Unit 1 reactor's graphite blocks (GR-280 grade graphite)			
No nitrogen impurities in graphite	–	$7.0\cdot10^{4*)}$	–
Minimal initial nitrogen impurities in graphite matrix	$1.8\cdot10^{4*)}$	$7.2\cdot10^{4*)}$	$5.2\cdot10^{4*)}$
Maximal initial nitrogen impurities in graphite matrix	$1.2\cdot10^{5*)}$	$5.0\cdot10^{5*)}$	$3.6\cdot10^{5*)}$
Maximal initial nitrogen impurities in graphite matrix and nitrogen is present in all open graphite pores	–	$8.6\cdot10^{5*)}$	–
Maximal initial nitrogen impurities in graphite matrix and nitrogen is present in all (open and closed) graphite pores	–	$9.9\cdot10^{5*)}$	–
Modelling of Ignalina NPP Unit 1 reactor's rings/sleeves graphite (GRP-2-125 grade graphite)			
No nitrogen impurities in graphite	$1.5\cdot10^{4*)}$	$6.1\cdot10^{4*)}$	$4.3\cdot10^{4*)}$
Maximal initial nitrogen impurities in graphite matrix**) and nitrogen is present in all open graphite pores	–	$6.5\cdot10^{5*)}$	–
Maximal initial nitrogen impurities in graphite matrix**) and nitrogen is present in all (open and closed) graphite pores	–	$6.8\cdot10^{5*)}$	–
Earlier modelling of Ignalina NPP Unit 1 reactor's graphite blocks (GR-280 grade graphite)			
Ref. [8] data, minimal initial impurities concentrations	–	–	$4.2\cdot10^4$
Ref. [8] data, maximal initial impurities concentrations	–	–	$3.4\cdot10^5$
Ref. [5] data	–	–	$5.0\cdot10^5$
Measurements of ChNPP Unit 2 reactor's graphite rings/sleeves (GRP-2-125 grade graphite)			
Ref. [14] data	$0.4\cdot10^4$	$2.8\cdot10^4$	$1.1\cdot10^4$
Measurements and modelling of various types reactors' graphite blocks and rings/sleeves			
Ref. [3], appendix F	$10^{3***)}$	$10^{6***)}$	$10^4–10^{5***)}$

*) – These activities are min., max. or avg. in axial direction in the region of the rector active core;
**) – Assuming the same concentration of nitrogen impurity as for GR-280 grade graphite – 70 ppm;
***) – Not exact values but only the order of magnitude.

2.2 Validation of modelling results using experimentally estimated (activity measurements of CPST) values

There was no published data on experimental investigations of Ignalina NPP RBMK-1500 reactors graphite radioactive inventory. However, first results of experimental investigation of ^{14}C specific activities in the irradiated RBMK-1500 reactors' graphite rings/sleeves (4 samples) were obtained by CPST (former Institute of Physics, Lithuania) in the course of the CARBOWASTE project [16]. Two samples (Gr.13 and Gr.14) were taken from the central part of the reactor core in the axial direction, while two others – Gr.18 and Gr.16 – from the top and the bottom parts (top and bottom reflectors) of the core respectively. Sample Gr.16 was the biggest and it was further divided into the smaller subsamples for subsequent determination of other radionuclides activities. The measurements were performed ~6 years after the time of withdrawal from the reactor (after the withdrawal from the reactor in 2003, the graphite rings were kept in the cooling pool until they were taken out for analysis after ~6 years of storage). More details about these samples (location, physical data, etc.) are presented in ref. [16].

2.2.1 Brief review of measurements and calculations made by CPST

The presented results [16] contained information about specific activities of ^{14}C in graphite rings/sleeves located in the regions of top reflector (one sample), bottom reflector (one sample) and active core (two samples) of the Ignalina NPP RBMK-1500 reactor. Estimated ^{14}C specific activities in the samples are presented in Table 4.

Table 4. Activities of ^{14}C in graphite rings/sleeves of RBMK-1500 reactor [16]

Sample code	^{14}C specific activity, Bq/g
Gr.18 (top reflector)	$(1.3\pm0.4)\cdot10^{4}$
Gr.13, Gr.14 (active core centre)	$(1.3\pm0.2)\cdot10^{5}$
Gr.16 (bottom reflector)	$(2.4\pm0.6)\cdot10^{4}$

The analysed samples were of not well known operation history and CPST developed a coupled method for estimation of irradiation history of the graphite samples. The proposed method employed modelled neutron fluxes in the graphite rings/sleeves at reactor operation and measured relations of $^{12}C/^{13}C$ nuclides quantities in the fresh and in the irradiated samples of graphite. It was estimated that analyzed irradiated graphite samples have been in the reactor core under irradiation for ~11.6 years at the reactor thermal power of 4200 MW. And then

finally, having these data and performing neutron activation modelling it was estimated that the experimentally measured specific activities of ^{14}C radionuclide corresponds to the initial nitrogen impurity content of ~15±4 ppm in the virgin rings/sleeves graphite. It should be noted that presence of ^{36}Cl in the sample of bottom reflector graphite Gr.16 was also investigated, but its activity was below detection limit of liquid scintillation counting technique.

The results of gamma spectrometry analysis of the sub-samples Gr.211, Gr.212 and Gr.213, which represent the inner surface of the bulk graphite sample Gr.16, as well as the results for the sub-samples Gr.221, Gr.222 and Gr.223, which represent the outer surface of the sample Gr.16 are summarized in Table 5.

Table 5. Activities of gamma emitters in graphite rings/sleeves of RBMK-1500 reactor [16]

Sample code	Specific activity, Bq/g						
	^{54}Mn	^{60}Co	^{134}Cs	^{137}Cs	^{152}Eu	^{154}Eu	^{155}Eu
Inner surface of Gr.16 sample							
Gr.211	1.5±0.2	350±50	<0.10	2.2±0.2	15.5±3.1	3.3±0.7	0.46±0.09
Gr.212	0.46±0.07	68±10	0.44±0.11	2.7±0.3	13.1±2.6	3.2±0.6	0.53±0.11
Gr.213	0.37±0.06	35±6	0.43±0.11	2.2±0.2	13.5±2.7	2.7±0.5	0.33±0.07
Outer surface of Gr.16 sample							
Gr.221	0.18±0.03	38±6	0.39±0.10	3.4±0.3	11.8±2.4	3.0±0.6	0.56±0.11
Gr.222	0.11±0.02	26±4	0.18±0.05	4.1±0.4	11.7±2.3	3.2±0.6	0.67±0.13
Gr.223	0.10±0.02	40±6	0.18±0.05	2.8±0.3	11.9±2.4	2.6±0.5	0.46±0.09
Average							
Average	$4.53\cdot10^{-1}$	$9.28\cdot10^{1}$	$2.85\cdot10^{-1*)}$	$2.90\cdot10^{0}$	$1.29\cdot10^{1}$	$3.00\cdot10^{0}$	$5.02\cdot10^{-1}$

*) – Calculated assuming that ^{134}Cs specific activity of Gr.211 sample is 0.09 Bq/g.

Results of actinides determination in the graphite rings/sleeves samples from the Ignalina NPP Unit 1 reactor were provided by CPST. Two samples (sub-sample of Gr.14 sample and sub-sample of Gr.16 sample, which represent active core centre and bottom reflector respectively) have been analyzed and obtained results are presented in Table 6.

Table 6. Activities of actinides in graphite rings/sleeves of RBMK-1500 reactor

Sample code	Specific activity, Bq/g				
	^{238}Pu	$^{239+240}Pu$	^{241}Am	^{242}Cm	$^{243+244}Cm$
Gr.14-2	$(400 \pm 70)\cdot10^{-3}$	$(70 \pm 20)\cdot10^{-3}$	$(120 \pm 50)\cdot10^{-3}$	$(90 \pm 30)\cdot10^{-3}$	11 ± 2
Gr.16-2	$(40 \pm 10)\cdot10^{-3}$	$(17 \pm 9)\cdot10^{-3}$	$(14 \pm 4)\cdot10^{-3}$	$(40 \pm 12)\cdot10^{-3}$	$(36 \pm 10)\cdot10^{-3}$

2.2.2 LEI modelling using impurities data obtained from measurements of irradiated graphite samples

Modelling of graphite rings/sleeves activation presented in this § 2.2.2 chapter is generally the same as conservative modelling cases (Cases A) for graphite rings/sleeves presented in Technical Report T-3.4.2 [4] with only one exception – initial maximal concentrations of several impurities are replaced with "explanatory" ones, derived from the experimental activity measurements of irradiated graphite samples. The analysed samples were irradiated from the beginning of Ignalina NPP Unit 1 reactor operation until August 2003, i.e. – almost until its final shutdown which was on the 31st December 2004. Also, CPST reported calculated irradiation period of irradiated graphite samples of ~11.6 years at the reactor thermal power of 4200 MW [16]. In terms of generated power this corresponds to generally whole lifetime of Ignalina NPP Unit 1 reactor at real operation history, so the irradiation history in this modelling case was also unchanged (it is presented in Technical Report T-3.4.2 [4]).

The "explanatory" initial concentrations of impurities were derived in reverse activation modelling way, similarly to the one presented in ref. [15]. I.e. the concentrations of impurities, which activation led to the generation of particular radionuclide, were altered until the modelled activity of that radionuclide (6 years after RFS) matched best the measured one. When the same impurity influenced activities of several measured radionuclides (and/or activities of the same radionuclide in different positions), the best match was obtained by the help of least squares method, i.e. the "explanatory" concentration was the one that gave the minimal sum of the squares of the differences between measured and modelled activities.

The "explanatory" concentrations were derived firstly for those impurities, which affect only one measured radionuclide activity at the time, and later for other impurities. For example, since both europium (Eu) and caesium (Cs) radionuclides are formed from a number of different light elements activation as well as from fission of actinides, their formation was analysed when the actinides concentrations were determined.

List of impurities and their "explanatory" concentrations which were defined according to the presented methodology, based on CPST radionuclides activity measurement results, are presented in the Table 7. Table 7 also contains data about measured quantities of listed impurities in virgin (unirradiated) GRP-2-125 graphite samples.

Table 7. List of impurities with their "explanatory" concentrations (weight fractions) and concentrations of these impurities reported in ref. [4] for virgin GRP-2-125 graphite

Element	"Explanatory" concentrations (%) defined according CPST activity measurements	Initial concentrations (%) reported in the ref. [4]
Ba	$4.76 \cdot 10^{-8}$	$2.01 \cdot 10^{-4}$
Co	$7.40 \cdot 10^{-9}$	$5.30 \cdot 10^{-6} - 9.00 \cdot 10^{-8}$
Cs	$1.16 \cdot 10^{-10}$	$4.90 \cdot 10^{-7} - 2.00 \cdot 10^{-8}$
Eu	$2.60 \cdot 10^{-12}$	$2.60 \cdot 10^{-7}$
Fe	$4.10 \cdot 10^{-4}$	$5.80 \cdot 10^{-3} - 1.00 \cdot 10^{-4}$
N	$1.30 \cdot 10^{-3}$	$4.60 \cdot 10^{-3} - 2.10 \cdot 10^{-4}$ *)
Nd	$7.36 \cdot 10^{-6}$	$1.10 \cdot 10^{-5}$
Ni	$3.90 \cdot 10^{-5}$	$3.90 \cdot 10^{-5} - 3.00 \cdot 10^{-5}$
Sm	$2.13 \cdot 10^{-11}$	$2.13 \cdot 10^{-6}$
Th	$8.40 \cdot 10^{-11}$	$8.40 \cdot 10^{-7} - 3.00 \cdot 10^{-8}$
U	$3.65 \cdot 10^{-7}$	$1.10 \cdot 10^{-5} - 1.60 \cdot 10^{-6}$

*) – Data taken from the Table 2 for GRP-2-125 graphite (no data for N in ref. [4] is reported).

Results of neutron activation modelling, obtained using these "explanatory" concentrations of impurities, presented in the Table 7, and maximal concentrations of all other remaining impurities from the ref. [4], together with the experimental measurements results for INPP Unit 1 reactor graphite rings/sleeves are presented in the Fig. 4 – Fig. 6 and Table 8 below.

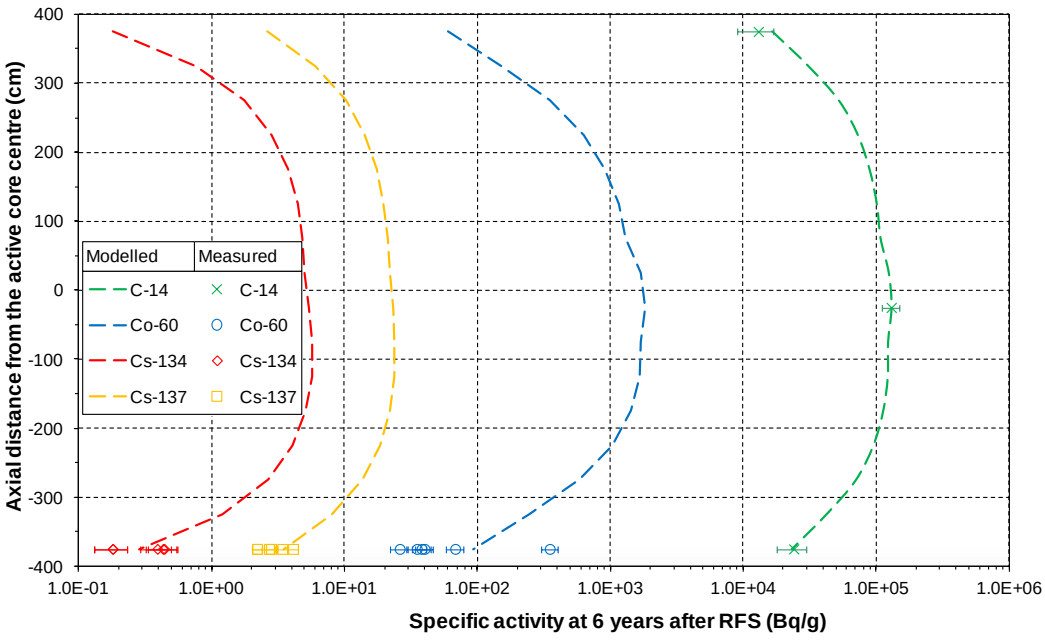

Fig. 4. Comparison of modelled and measured specific activities of ^{14}C, ^{60}Co, ^{134}Cs and ^{137}Cs in the graphite rings/sleeves of RBMK-1500 reactor at 6 years after RFS

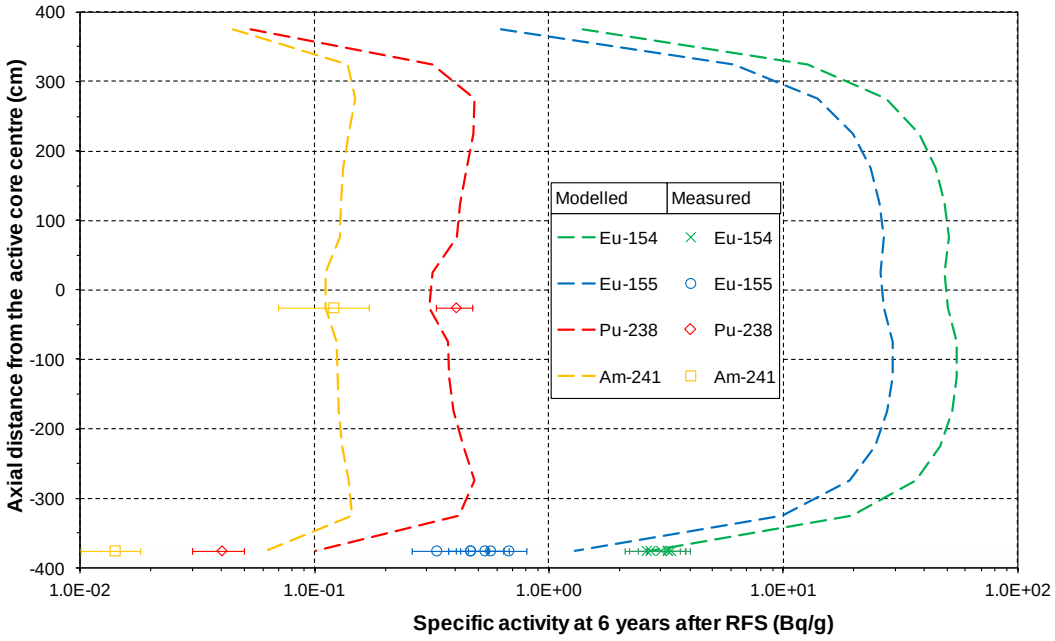

Fig. 5. Comparison of modelled and measured specific activities of ^{154}Eu, ^{155}Eu, ^{238}Pu and ^{241}Am in the graphite rings/sleeves of RBMK-1500 reactor at 6 years after RFS

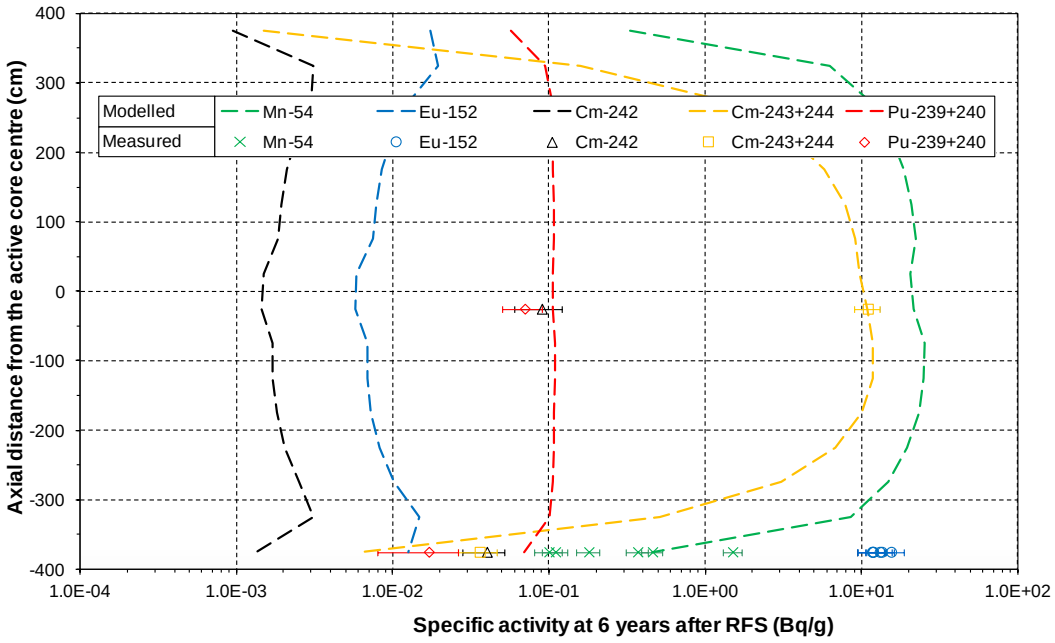

Fig. 6. Comparison of modelled and measured specific activities of ^{54}Mn, ^{152}Eu, $^{239+240}$Pu, ^{242}Cm and $^{243+244}$Cm in the graphite rings/sleeves of RBMK-1500 reactor at 6 years after RFS

Table 8. Modelled and measured radionuclides specific activities in the graphite rings/sleeves of RBMK-1500 reactor at 6 years after RFS

Radionuclide	Measured specific activity, Bq/g	Modelled specific activity, Bq/g
^{14}C (top reflector)	$1.30 \cdot 10^{4}$	$1.66 \cdot 10^{4}$
^{14}C (active core centre)	$1.30 \cdot 10^{5}$	$1.30 \cdot 10^{5}$
^{14}C (bottom reflector)	$2.40 \cdot 10^{4}$	$2.32 \cdot 10^{4}$
^{54}Mn	$4.53 \cdot 10^{-1}$ (average)	$4.57 \cdot 10^{-1}$
^{60}Co	$9.28 \cdot 10^{1}$ (average)	$9.30 \cdot 10^{1}$
^{134}Cs	$2.85 \cdot 10^{-1*)}$ (average)	$2.85 \cdot 10^{-1}$
^{137}Cs	$2.90 \cdot 10^{0}$ (average)	$3.47 \cdot 10^{0}$
^{152}Eu	$1.29 \cdot 10^{1}$ (average)	$1.26 \cdot 10^{-2}$
^{154}Eu	$3.00 \cdot 10^{0}$ (average)	$2.71 \cdot 10^{0}$
^{155}Eu	$5.02 \cdot 10^{-1}$ (average)	$1.29 \cdot 10^{0}$
^{238}Pu (active core centre)	$4.00 \cdot 10^{-1}$	$3.09 \cdot 10^{-1}$
^{238}Pu (bottom reflector)	$4.00 \cdot 10^{-2}$	$1.01 \cdot 10^{-1}$
$^{239+240}$Pu (active core centre)	$7.00 \cdot 10^{-2}$	$1.06 \cdot 10^{-1}$
$^{239+240}$Pu (bottom reflector)	$1.70 \cdot 10^{-2}$	$6.93 \cdot 10^{-2}$
^{241}Am (active core centre)	$1.20 \cdot 10^{-1}$	$1.11 \cdot 10^{-1}$
^{241}Am (bottom reflector)	$1.40 \cdot 10^{-2}$	$6.21 \cdot 10^{-2}$
^{242}Cm (active core centre)	$9.00 \cdot 10^{-2}$	$1.45 \cdot 10^{-3}$
^{242}Cm (bottom reflector)	$4.00 \cdot 10^{-2}$	$1.33 \cdot 10^{-3}$
$^{243+244}$Cm (active core centre)	$1.10 \cdot 10^{1}$	$1.09 \cdot 10^{1}$
$^{243+244}$Cm (bottom reflector)	$3.60 \cdot 10^{-2}$	$6.14 \cdot 10^{-3}$

*) – See explanation under the Table 5.

2.2.3 Results and discussion

Comparison of the modelled specific activities of ^{14}C in the graphite rings/sleeves in the region of active core, top and bottom reflectors (using estimated "explanatory" 13 ppm initial concentration of nitrogen impurity) shows very good agreement with the measured, as presented in Fig. 4 and Table 8. Modelled specific activities of ^{14}C are the same as measured ones (including measurement errors):

- ~$1.30 \cdot 10^{5}$ Bq/g in the graphite rings/sleeves in the region of active core, while measured activity is ~$1.3 \pm 0.2 \cdot 10^{5}$ Bq/g;
- ~$1.66 \cdot 10^{4}$ Bq/g in the graphite rings/sleeves in the region of top reflector, while measured activity is ~$1.3 \pm 0.4 \cdot 10^{4}$ Bq/g;

- ~$2.32 \cdot 10^4$ Bq/g in the graphite rings/sleeves in the region of bottom reflector, while measured activity is ~$2.4 \pm 0.6 \cdot 10^4$ Bq/g.

Furthermore, in § 2.1.2 chapter derived equation (3) for the analytical evaluation of maximal ^{14}C specific activity in the graphite rings/sleeves in the gives the same result as modelling – inserting 13 ppm of nitrogen impurities in this equation gives ~$1.30 \cdot 10^5$ Bq/g specific activity of ^{14}C in the graphite rings/sleeves at RFS. CPST also reported calculated nitrogen impurity of 15±4 ppm which gives closest results of their modelling in comparison with measurements. This quantity of 15±4 ppm for nitrogen is also in good agreement with here determined "explanatory" concentration of 13 ppm nitrogen. There is no published data on initial nitrogen impurity content in GRP-2-125 grade graphite, but estimated "explanatory" concentration (13 ppm) is less than possible maximal calculated concentration of nitrogen in graphite pores (46 ppm, see Table 7) and less than maximal reported concentration for GR-280 grade graphite (70 ppm, see Technical Report T-3.4.2 [4]).

Results of modelled and measured activities of ^{54}Mn, ^{60}Co, ^{134}Cs, ^{137}Cs and ^{154}Eu radionuclides also agree very well (see Fig. 4 – Fig. 6 and Table 8), i.e. taking into account the errors of measurements, the modelled specific activities of these radionuclides coincide with the measured. The measured and modelled specific activities of ^{155}Eu, ^{238}Pu, $^{239+240}Pu$, ^{241}Am and $^{243+244}Cm$ radionuclides differ not more than 6 times, so agreement of modelling and measurements still may be considered as good, see Fig. 5, Fig. 6 and Table 8. The biggest inconsistencies are observed for ^{242}Cm and ^{152}Eu radionuclides, where measured specific activities are respectively up to ~60 and ~$1 \cdot 10^3$ times higher than the modelled activities (see Fig. 6 and Table 8).

Estimated "explanatory" concentrations of impurities – Ba, Co, Cs, Eu, Fe, Nd, Sm, Th and U, which activation led to the production of earlier mentioned radionuclides (except ^{14}C), are less than reported maximal concentrations in the Technical Report T-3.4.2 [4] (also see Table 7). The only exception is Ni, which maximal concentration was set as "explanatory".

Summarising information and results presented in this § 2.2 chapter it may be concluded, that using "explanatory" impurities concentrations, which were derived in reverse activation modelling way, modelled specific activities of all measured radionuclides are in good agreement with the measurement results (with exception of ^{152}Eu and ^{242}Cm radionuclides).

The calculated "explanatory" concentrations are also less (or equal) than maximal reported initial concentrations for all impurities. All this also generally confirms the hypothesis that "real" specific activities of radionuclides are somewhere in the range of modelling results, obtained using maximal and minimal initial concentrations of impurities. Furthermore, good agreement of modelled and measured specific activities of ^{14}C radionuclide at the different heights of reactor core (as well as similar tendencies for actinides) indicates that axial distribution of neutron fluxes in the graphite structures was modelled adequately.

However, it should be noted that numerical modelling of induced activity in the graphite components, presented in this report, does not take into account two processes – the possible release of emerged radionuclides from the graphite to the surrounding material/atmosphere and opposite process – uptake of radionuclides from the surrounding material/atmosphere. These two processes depending on various conditions may be important to the whole balance of particular radionuclide in the graphite components, but they cannot be directly modelled with the computer codes, used for estimation of induced activity.

For example, it is broadly agreed, that one of the most important pathways of ^{14}C (and others) radionuclide release from the graphite during reactor operation is associated with radiolytic corrosion of the graphite. However, this process is specific for CO_2 cooled reactors, such as UNGG, MAGNOX, etc. The RBMK reactor graphite stack operates in nitrogen-helium gas mixture to prevent the oxidation and the presence of CO and CO_2 in this cooling gas mixture is limited and controlled – maximal allowable $CO+CO_2$ volumetric fraction at reactor operation is less that 0.02 % [11, 12]. So this mechanism for RBMK is not so important, however should not be totally excluded. Additionally, special account should be made to the fact that here analysed irradiated RBMK graphite samples until analysis were kept in the cooling pool in the Reactor Building. During the ~6 years storage period in the water, the release of radionuclides by leaching could occur and consequently measured radionuclides activities might be lower. On the other hand, the water of cooling pool is contaminated with various radionuclides and opposite process – uptake of radionuclides into the graphite could occur during the storage period and this might increase measured radionuclides activities.

So, all these phenomena should be not forgotten when comparing and explaining the measured and the modelled radionuclides inventories in the irradiated RBMK reactor graphite samples.

2.3 Conclusions

The performed analysis of possible ^{14}C production in RBMK-1500 reactor graphite could be summarised identifying that:

- Activity of ^{14}C produced from carbon (raw graphite material) activation is in the order of 10^4 Bq/g and its axial distribution corresponds to the thermal neutron flux distribution;
- Production of ^{14}C from activation of initial nitrogen impurities in graphite matrix is linearly proportional to its quantity and at nitrogen concentration of ~$1 \cdot 10^{-3}$ % mass, ^{14}C production from nitrogen activation equals the one from carbon activation;
- The very conservative estimation of possible nitrogen penetration from the cooling gasses into the graphite pores revealed, that nitrogen content in the graphite pores may be in the order of magnitude up to the 10^{-3} % of initial graphite mass (which is comparable to the maximal reported nitrogen impurity in the graphite matrix) and this may significantly influence total produced ^{14}C activity in graphite.

Validation of modelled specific activities of measured radionuclides was performed employing adjustment of initial concentrations of impurities in order to get the modelled specific activities as close as possible to the measured ones and comparing adjusted concentrations to the experimentally obtained for virgin graphite. The performed evaluation shows that:

- Modelled radionuclides specific activities in the graphite rings/sleeves using estimated "explanatory" concentrations of impurities show good agreement with the measured, as modelled specific activities fall in the range of (or are close to) measured taking into account measurement uncertainties (except ^{152}Eu and ^{242}Cm);
- The calculated "explanatory" concentrations for all impurities are less (or equal) than published maximal concentrations of impurities in virgin graphite.

3 Romania

3.1 Isotopes accumulation in TRIGA MTR graphite

This § 3 chapter presents results of preliminary and updated numerical evaluation of nuclides accumulation in the thermal column of TRIGA Materials Test Reactor at INR, Pitesti.

3.1.1 Modelling tools

The modelling tools used for the assessment of the radionuclide content in the graphite irradiated in the thermal column of TRIGA reactor were:

- WIMS (cell transport code) for cross section generation;
- DFA (system of 3D core codes with burnup loop) for flux and power distribution;
- ORIGEN-S (SCALE 5 system burnup code) for nuclide activities, densities evaluation.

3.1.2 Model hypothesis and main general input data

The geometry and configuration of the TRIGA INR reactor is presented in Fig. 7.

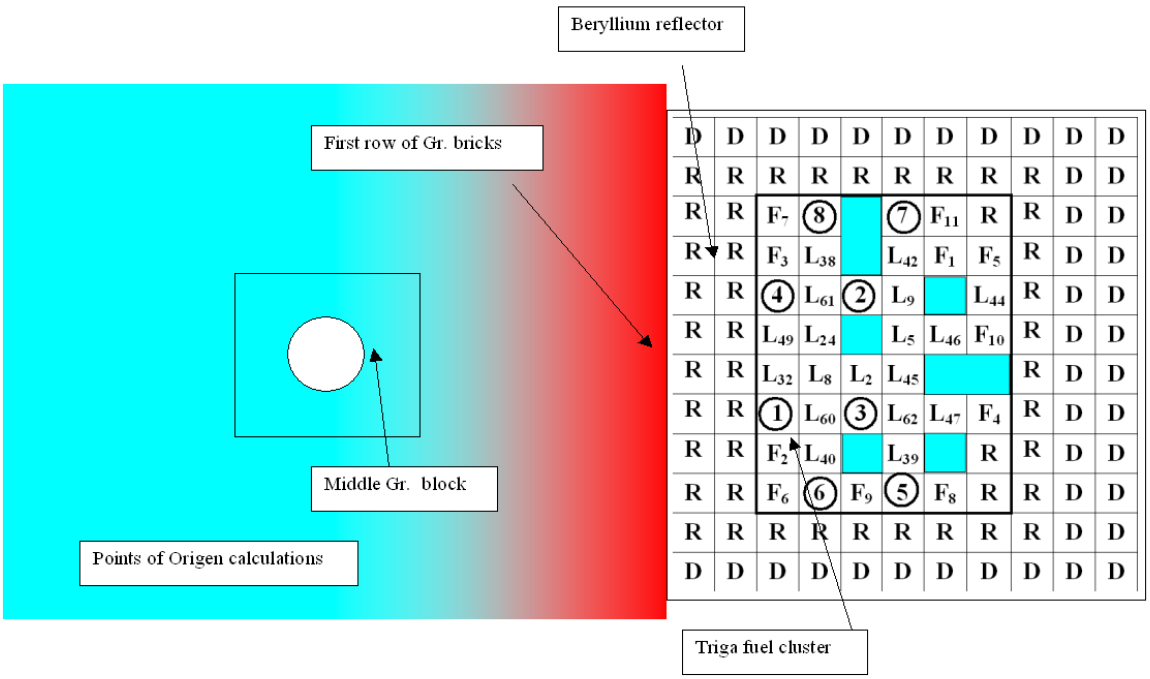

Fig. 7. General geometry layout used for neutronic calculations of the TRIGA reactor

Burnup modelling was carried out considering 10 MW average reactor power using real energy history. Thermal column was modelled according to its real geometry and working conditions:

- Column size: 172 × 114 × 71 cm^3;
- Number of graphite bricks: 96 (12 rows of 8 bricks);
- Graphite block size: 14.3 × 14.3 × 71 cm;
- Distance from the reactor core: 25 cm;
- Beryllium wall width: 17.78 cm;
- Irradiation time and power: 10 years at 10 MW;
- Time after the termination of irradiation (decay): 10 years.

3.1.3 Summary of preliminary simulation

The details of preliminary calculation may be found in ref. [17]. The main data, i.e. neutron flux and material composition used for simulation were as follow:

- Neutron flux:
  - Flux (thermal): $6.9 \cdot 10^{10}$ nv;
  - Flux (epithermal): $1.1 \cdot 10^{8}$ nv;
  - Flux (fast): $4.0 \cdot 10^{6}$ nv.
- Impurities content:
  - Experimentally determined by XRF (see ref. [17]).

The activities of some emerged radionuclides from the activation and fission reactions of carbon and XRF measured impurities are listed in the Table 9.

Table 9. Predicted vs. measured radionuclides activities

Radionuclide	Predicted activity (Bq/g)	Measured activity (Bq/g)
^{3}H	$1.23 \cdot 10^{-10}$	$(0.7–2.0) \cdot 10^{4}$
^{14}C	$1.01 \cdot 10^{2}$	$(0.8–1.9) \cdot 10^{3}$
^{60}Co	–	$(1.7–6.9) \cdot 10^{1}$
^{152}Eu	$1.30 \cdot 10^{-7}$	$(0.5–1.9) \cdot 10^{3}$
^{154}Eu	$4.66 \cdot 10^{-6}$	$(0.3–1.2) \cdot 10^{2}$

The comparison of modelled values with measured (Table 9) led to the following conclusions:

- Large amount of ^{3}H measured can be justified only by the activation of light elements (as lithium (Li)) at impurity level;
- ^{14}C activity predicted from ^{13}C activation is also underestimated compared to the measured values, suggesting that activation of nitrogen (N) adsorbed on the particle surface brings an important contribution and must be considered;
- ^{152}Eu and ^{154}Eu activities resulted from fission and activation of Th and Dy impurities do not match neither the activities measured in the graphite block, nor the ratio $^{152}Eu/^{154}Eu$, indicating that Eu as impurity, even at ppb level, has to be considered;
- ^{60}Co is not predicted by simulation if cobalt (Co) as impurity is neglected.

3.1.4 Simulations using updated input data based on activity measurements

Adding lithium (Li), nitrogen (N), cobalt (Co) and europium (Eu) as impurities in the graphite content for activation modelling, large sensitivity in activity of ^{3}H, ^{14}C, ^{60}Co, ^{152}Eu and ^{154}Eu was observed (note, that Li, N, Eu and Co were not measured by the XRF techniques used at INR).

Using N concentration measured by EDS (0.01 %wt) and measured $^{152}Eu/^{154}Eu$ ratio, the irradiation flux leading to measured ^{14}C activity had to have the following characteristics:

- Flux (thermal): $1.7 \cdot 10^{11}$ nv;
- Flux (epithermal): $9.5 \cdot 10^{8}$ nv;
- Flux (fast): $8.2 \cdot 10^{7}$ nv.

For this neutron flux, Li, Eu and Co concentrations were determined based on the neutron activation approach (Table 10).

Table 10. Impurities assessed by inverse neutron activation approach

Impurities	N	Eu	Li	Co
Concentration (g/kg C)	0.1	$7.0 \cdot 10^{-6}$	$6.2 \cdot 10^{-5}$	$3.0 \cdot 10^{-6}$
Comments	Measured by EDS	Calculated by neutron activation		

Then radionuclide accumulation in different locations of the thermal columns has been calculated for the following cases:

Case A

- Neutron flux: determined as optimum flux matching measured ^{14}C activity and $^{152}Eu/^{154}Eu$ ratio;
- Impurities content: experimentally determined by XRF (see ref. [17]) plus N measured by EDS, and Eu, Li and Co calculated based on inverse neutron activation (Table 10).

Case B

- Neutron flux: corresponding to the geometrical centre of the column:
  - Flux (thermal): $5.0 \cdot 10^{10}$ nv;
  - Flux (epithermal): $0.9 \cdot 10^{8}$ nv;
  - Flux (fast): $3.2 \cdot 10^{6}$ nv.
- Impurities content: as for Case A.

Case C

- Neutron flux: corresponding to the centre of the first row next to the active zone (maximum flux):
  - Flux (thermal): $2.0 \cdot 10^{13}$ nv;
  - Flux (epithermal): $2.6 \cdot 10^{12}$ nv;
  - Flux (fast): $3.79 \cdot 10^{11}$ nv.
- Impurities content: as for Case A.

3.1.5 Results

Case A

The radioactive elements resulted from the activation and fission reactions of carbon (C) and the assumed impurities are listed in Table 11.

For the listed radionuclides the predicted activities (Case A, Table 11) fall in the range of the measured values, except ^{154}Eu which is overestimated. Also, the ratio $^{152}Eu/^{154}Eu$ (10.2) is lower than the value obtained from the measured activities which ranges from 12 to 18.

Table 11. Comparison of radionuclides activities for different positions in the thermal column

Radionuclide	Predicted Activity (Bq/g)			Measured activity (Bq/g)
	Column centre Case B	Sample location Case A	First row Case C	
^{3}H	$2.87 \cdot 10^{3}$	$9.73 \cdot 10^{3}$	$3.89 \cdot 10^{5}$	$(0.7–2.0) \cdot 10^{4}$
^{14}C	$2.82 \cdot 10^{2}$	$9.58 \cdot 10^{2}$	$1.12 \cdot 10^{5}$	$(0.8–1.9) \cdot 10^{3}$
^{60}Co	$7.79 \cdot 10^{0}$	$2.66 \cdot 10^{1}$	$2.87 \cdot 10^{3}$	$(1.7–6.9) \cdot 10^{1}$
^{152}Eu	$5.40 \cdot 10^{2}$	$1.62 \cdot 10^{3}$	$2.40 \cdot 10^{0}$	$(0.5–1.9) \cdot 10^{3}$
^{154}Eu	$4.70 \cdot 10^{1}$	$1.59 \cdot 10^{2}$	$2.74 \cdot 10^{3}$	$(0.3–1.2) \cdot 10^{2}$

Case B

Smaller neutron flux corresponding to the centre of the thermal column lead to the lower radionuclides activities (see Case B in the Table 11).

Case C

The maximal neutron flux determined higher activities (see Case C in the Table 11), especially for ^{3}H due to the fast neutrons in the spectrum.

3.1.6 Conclusions

Table 11 shows that the sample measured was placed somewhere between the margin and the centre of the column, towards the reactor core.

Uncertainties on impurity content

Presence of very small content of lithium (Li) explains high activity of ^{3}H but experimental evidences are needed to prove it.

Only the existence of europium (Eu) as impurity, even at very low level, can explain the measured activities and the ratio $^{152}Eu/^{154}Eu$.

^{14}C activity is sensitive to nitrogen (N) content and future measurements are needed to support the value used in the TRIGA thermal column activation calculations.

Uncertainties on irradiation conditions

Radionuclide content depends on the position in the thermal column due to the variation of the neutron flux. While thermal column model can predict accurately the value of the flux along the thermal column, position of the graphite block used in the experimental measurements is unknown. Moreover, it could have had different position inside the thermal column during all irradiation period. This can explain the differences between the predicted and measured values.

4 United Kingdom

4.1 Development of an experimental and simulation process to determine the end of life radionuclide inventory of UK irradiated graphite waste

4.1.1 Introduction

The UK has predominantly used graphite moderated reactors for research purposes and both the production of electricity and weapons material, consequently the Nuclear Decommissioning Authority (NDA) has estimated when all reactors are shutdown this will represent a graphite waste legacy of 99000 tonnes [18, 19]. Graphite wastes are known to contain a wide range of radionuclides, including ^{3}H, ^{14}C and ^{60}Co, which arise from both activation of impurities present in the graphite at start of life and from contamination from other components in the reactor circuit. The majority of this material will be classified as Intermediate Level Waste (ILW), a category which the UK does not currently have a disposal route for [20]. The preferred option under consideration for ILW is disposal in a deep geological repository, however graphite wastes would account for 33 % of any repository volume [19]. Therefore innovative treatment options are under investigation which may provide methods to remove a significant proportion of this activity thus reducing the bulk of the material from ILW to Low Level Waste (LLW); considerably reducing the disposal cost and volume [21]. To inform both direct disposal and possible treatment options will require accurate predictions of the end of life activity of the waste. As it would be impractical to perform large scale characterisation of the graphite, it is the aim of this work to develop models to predict the inventory. These models are developed at the University of Manchester (UoM) using both reactor physics and activation codes and the results compared against experimental analysis performed at the UoM on samples which have been trepanned from reactor cores.

NNL modelling

National Nuclear Laboratory (NNL) also performed similar activation modelling for Oldbury and Wylfa MAGNOX reactors graphite in UK within the scope of WP2 of CARBOWASTE project. However, their modelling purpose is more related to the evaluation of potential radiological situation for planning of deconstruction of graphite cores. The short summary of

this work is presented below whereas full report is available as CARBOWASTE project Deliverable D-2.3.1D [22].

For planning purposes prior to deconstruction of the graphite cores it is important to be able to model the expected inventory in the graphite. As the movement of radionuclides around the core and from failed fuel is a probabilistic process it is not beneficial to consider these effects at this stage and thus this report studies only the activation of elements present in the graphite at manufacture.

Currently the most practical method of justifying the accuracy of activation calculations is to benchmark calculations against experimental measurements. This study reports comparison between calculation and measurements of the activation products in four graphite samples to help justify the accuracy of such calculations for decommissioning purposes.

The results show that it is possible to predict the ^{14}C content of the four graphite samples to within a factor of four by assuming the 10 ppm of nitrogen given in the PGA specification, precise alignment of the results with measurements would require the Oldbury graphite initially to contain 100 ppm of nitrogen and the Wylfa graphite to contain no nitrogen. There is however some evidence that the Wylfa sample's surface deposits contains more ^{14}C than found in the bulk of the sample suggesting this (or some of its precursors) may be more mobile that the carbon initially in the graphite.

The ^{36}Cl found in the Oldbury samples is about 20 times over-estimated when compared to the FISPIN calculations and in the Wylfa samples about 5 times. Apart from the nuclear data and flux modelling within the codes, two potential explanations for this would be the initial chlorine content of the graphite is much lower that assumed in this work or that the initial chlorine and/or the ^{36}Cl product may be being lost from the graphite during the irradiation.

The other nuclides calculated show a very large variation in the calculated/experimental (C/E) values, possibly due to the uncertainty and variability of initial elemental impurities, nuclides being lost from the graphite during irradiation, or nuclides being deposited onto (or into) the samples from elsewhere in the core (e.g. activation of pipe work or from burst cartridges).

4.1.2 Modelling methodology

During the operational life of both MAGNOX and AGR reactors samples are periodically trepanned from graphite bricks for core integrity studies, these samples may also be analysed for radionuclide content. This combined with accurate information regarding the fuel rating in the channel provides sufficient data for both the development and validation of radionuclide inventory calculations. Given that the lifetime behaviour of graphite components in a nuclear reactor is complex with both structural and compositional changes [23] the development of the calculations in this study has been split into three stages:

- Stage 1: Calculations in this stage consider an isolated system, where the original impurities in the graphite are the only possible source of activation, there is no contamination or removal of material from the system;
- Stage 2: Calculations in this stage will take into account radiolytic oxidation of the graphite, representing loss of material from the system;
- Stage 3: Representing a fully dynamic system, where account is taken of possible contamination of the graphite from other material in the reactor circuit such as the fuel, clad, coolant and other structural components.

The work described in this study represents Stage 1 type calculations. A trepanned sample of mass 4.35 g has been obtained from the Wylfa 1 MAGNOX reactor and examined in the active facilities at the University of Manchester. The Wylfa Reactor 1 was commissioned in 1971, the core is constructed of Pile Grade A (PGA) graphite moderator bricks, with 6156 vertical fuel channels containing 49248 fuel elements. This particular sample was trepanned in April 2007 from fuel channel 1319, and had experienced an average lifetime fuel rating of 2.88 MW/t. The ^{3}H and ^{14}C content of the sample were measured using liquid scintillation beta counting and the ^{60}Co content using a NaI(Tl) gamma spectrometer. In order to use reactor physics codes to simulate the radionuclide inventory of irradiated graphite samples information is required in four areas:

1. Elemental composition of the graphite before irradiation;
2. Neutron flux experienced during lifetime;

3. Reaction cross-sections for the elements present;
4. Decay pathways of the resultant radionuclides.

PGA graphite is manufactured from a petroleum coke and coal tar binder [24] and involves several high temperature baking (~800 ^{o}C), graphitising (~2800 ^{o}C) and purification stages which remove most of the impurities, however it is inevitable that trace impurities remain, additionally compounds used in the manufacturing process lead to further contamination of the final product [25, 26]. Historic information regarding the original impurity content of PGA graphite is limited, current simulations use information from a study undertaken by White et al. in 1984 using mass spectrometry of the ash residue of UK graphite grades [27], the derived composition from this study is detailed in Table 12.

Table 12. Impurity content of PGA graphite, experimentally determined by White et al., in 1984 [27]

Impurity element	PGA (ppm)	Impurity element	PGA (ppm)	Impurity element	PGA (ppm)
Li	0.05	Ti	3	Cd	0.04
Be	0.02	V	12	In	0.05
B	0.1	Cr	0.35	Sn	0.05
N	10	Mn	0.04	Ba	1.5
Na	1.0	Fe	10	Sm	0.04
Mg	0.1	Co	0.02	Eu	0.004
Al	1.0	Ni	1.0	Gd	0.005
Si	35	Zn	0.13	Dy	0.008
S	50	Sr	0.4	W	0.12
Cl	2.0	Mo	0.1	Pb	0.12
Ca	35	Ag	0.001	Bi	0.08

The ANSWERS software code WIMS9A [28] was used to calculate the neutron flux (n/cm^2) in the graphite moderator. The model is a two-dimensional “pin-cell” of a single fuel channel surrounded by a reflective boundary representing whole core conditions. The calculation involves a burn-up cycle to simulate the fuel performance at mid-life, an average of two years for MAGNOX fuel. The neutron flux averaged over the entire graphite moderator brick was output using 172 energy group structure which is shown in Fig. 8.

The inventory calculation is performed using the United Kingdom Atomic Energy Authority (UKAEA) neutron activation software FISPACT [29].

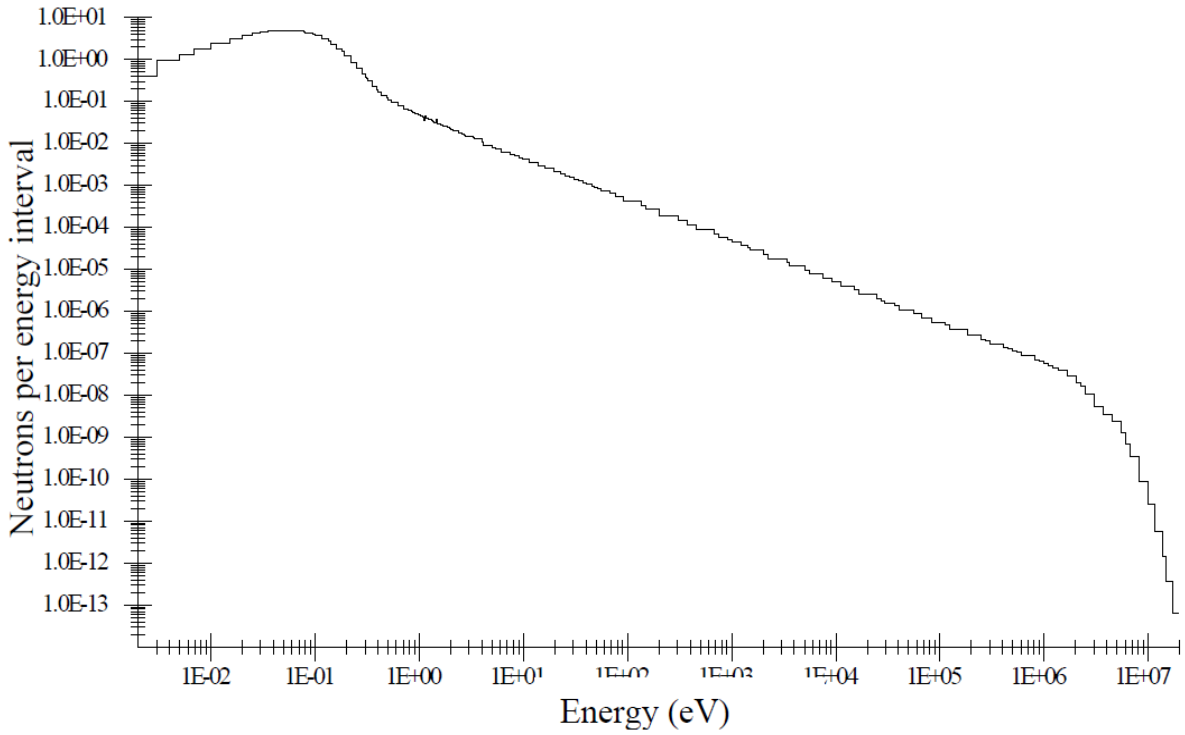

Fig. 8. Normalized neutron flux in graphite in 172 energy groups for MAGNOX fuel at mid-life, calculated using the WIMS9 code

This software uses the 2007 version of the European Activation Files (EAF), which contains an extensive data library of 65565 neutron induced cross-sections and a database of decay information for 2231 nuclides [29]. This software is used to determine the result of exposure of a group of elements to a neutron flux, integrating this over a specified time period and calculating the final activity and production pathways. These simulations outlined the sample to have a mass 4.35 g and density 1.74 g/cm^3, with elemental composition as detailed in Table 12. In addition the operational and shutdown times of the reactor are included in the calculation, this is particularly important if a precursor nuclide has a short decay time whereby it would decay during the shutdown period before it can undergo further neutron activation. For this reason the FISPACT simulation can incorporate shutdown times for the reactor by setting the flux at these time intervals to zero.

4.1.3 Discussion

The experimental and simulated results are compared in Table 13 and show that the calculated results are greater than the experimental values in all cases. The calculated activities ranged

from 36 % for ^{14}C, 24 % for ^{60}Co and 120 % for ^{3}H, which, considering the uncertainties, are reasonable close for this type of comparison. The predictions also show that the quantities of the impurity elements assumed to be present, based on historic data, at start of life are sufficient to account for the experimentally determined end of life activity of the sample before including any additional contamination which may come from the reactor circuit.

The primary source of uncertainty in the results is recognised to arise from the impurity composition. The impurity levels can have a significant effect on the quantity of radionuclide produced; in addition, for ^{3}H, it is reasonable to assume that, given the high mobility, a considerable fraction of the original activity may be lost before, or during experimental analysis [30, 19, 23].

Table 13. Comparison of experimental and simulated results for ^{3}H, ^{14}C and ^{60}Co, for Wylfa sample 1319/12

	Experimental		Simulation	
Radionuclide	**Activity (Bq/g)**	**Uncertainty (%)**	**Activity (Bq/g)**	**C/E**
^{3}H	$2.08 \cdot 10^{5}$	10	$4.57 \cdot 10^{5}$	2.20
^{14}C	$5.09 \cdot 10^{4}$	10	$6.93 \cdot 10^{4}$	1.36
^{60}Co	$2.37 \cdot 10^{4}$	5	$2.93 \cdot 10^{4}$	1.24

The calculated production pathways from FISPACT are given in Table 14 and illustrate that both Tritium and ^{60}Co are produced from single precursor elements; ^{6}Li and ^{59}Co respectively. ^{14}C is produced via ^{13}C and ^{14}N, with an approximately 50/50 split between these two routes. This latter finding is an important result as there is currently debate [31] about which of these reactions is the predominant route for ^{14}C production in irradiated graphite waste.

Table 14. Relative percentage of production pathways from original elements in graphite to ^{3}H, ^{14}C and ^{60}Co

Radionuclide	Production pathway	Relative contribution (%)
^{3}H	^{6}Li (n,a) ^{3}H	99.461
	^{6}Li (n,a) ^{3}H (b-)^{3}He(n,p) ^{3}H	0.508
^{14}C	^{14}N (n,p) ^{14}C	48.522
	^{13}C(n,γ) ^{14}C	51.476
^{60}Co	^{59}Co (n, γ) ^{60}Co	42.483
	^{59}Co (n, γ) ^{60m}Co (IT) ^{60}Co	53.163

The relative cross-sections for ^{14}C production reactions are given in Table 15; for a 1 % concentration of ^{13}C the reaction cross-section is 0.0009 barns and 0.001 % ^{14}N inclusion the cross-section is 1.8 barns. When considering the relative ratio of the abundance of both species within this virgin nuclear graphite this is inversely proportional to the ratio of the cross-sections therefore an almost equal contribution per reaction pathway for the production of ^{14}C is expected. This result is regardless of any net gain or loss, as is the case for this isolated system under consideration.

Table 15. Abundance and cross-section information for ^{14}C production routes [23]

Reaction	Abundance of isotope in natural element (%)	Cross-section of reaction (barns)
^{14}N (n,p) ^{14}C	99.63	1.8
^{13}C(n,γ) ^{14}C	1.07	0.0009

4.1.4 Conclusions

Predictions of the end of life activity of ^{3}H, ^{14}C and ^{60}Co for MAGNOX graphite have been performed and compared against experimental results obtained from a trepanned sample taken from a moderator brick in the Wylfa Reactor 1. These predictions show good agreement for ^{14}C and ^{60}Co. The differences between the experimental and calculated results may be due to the assumed original impurity levels for the virgin graphite which were obtained from historic data. In addition, these calculations only take into account the original impurity content, whereas the behaviour of graphite in the core may include both loss of material, via radiolytic oxidation, and gain of impurities via contamination from other material in the reactor circuit. Future plans for this research include using mass spectrometry analysis to determine the impurity content of UK graphite grades: PGA and Gilsocarbon, as well as extensive sensitivity studies on the input data. The complexity of the models will also be expanded to reflect the dynamic processes experienced by the graphite in the core environment.

5 France

5.1 EDF graphite and radionuclide inventory

5.1.1 EDF graphite

A short summary of the origins of EDF graphite is presented in this § 5.1 chapter. More details can be found in a CARBOWASTE project Deliverable D-1.1.4 [32].

EDF was in France the operator of six gas-cooled reactors, all shutdown now (see Fig. 9). They will have to be dismantled as soon as possible, and at least by 2022 for the retrieval of the first graphite brick from the Bugey 1 reactor. These reactors are of so-called in French, "UNGG" reactor type. They were graphite moderated, cooled by carbon dioxide and fuelled with natural uranium. The design of UNGG reactors is, in its general principle, very close to that of the British MAGNOX reactors, that was developed independently.

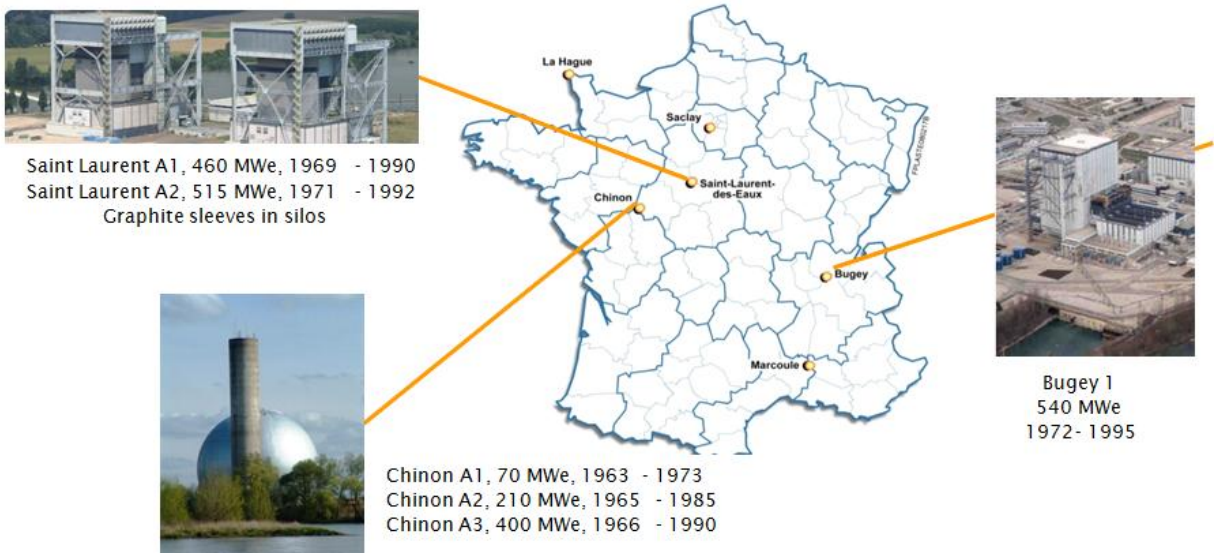

Fig. 9. Location of EDF irradiated graphite in France

Concerning graphite in UNGG reactors, this material was used in different parts of the reactors as a moderating element in the core, as mechanical support of the fuel cartridge in the fuel channels of the pile (graphite sleeves) and also as a biological shield under the pile in the case of the so-called integrated vessel reactors (Saint-Laurent A1 & A2, Bugey 1). A scheme of the main possible uses of graphite in UNGG reactors is shown in Fig. 10. The irradiated graphite

still lies in the reactors or is stored in silos for the sleeves which are not already shipped (see Fig. 9).

The total amount of irradiated graphite for EDF UNGG reactors is about 17 000 t. It consists of 13 000 t of graphite bricks from the piles of the six UNGG reactors, 2 000 t of graphite sleeves in silos in Saint-Laurent and 2 000 t of graphite used as biological shield under the core of integrated vessel type reactors.

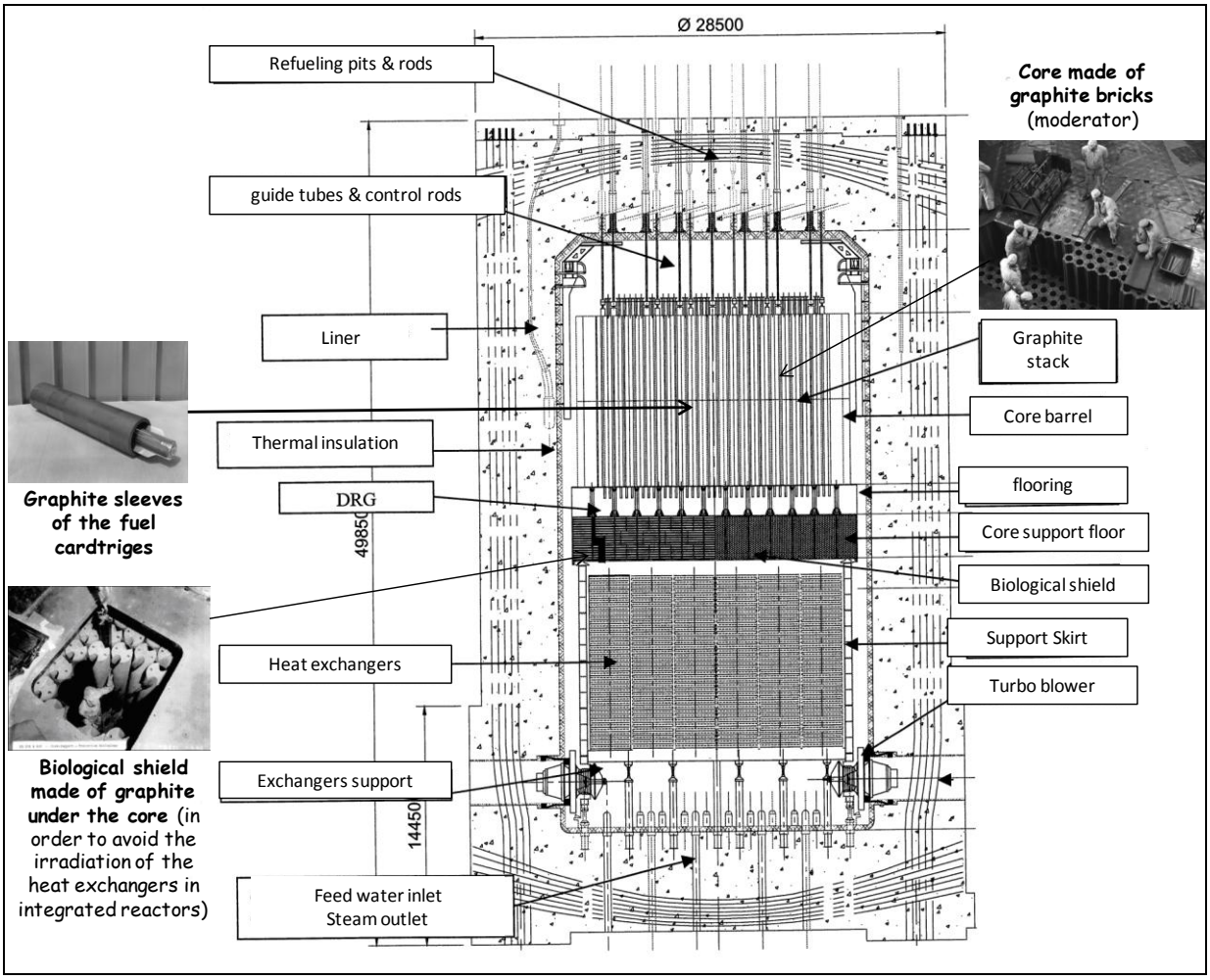

Fig. 10. Main possible uses of graphite (depending on the reactor design) in EDF UNGG reactors

5.1.2 The purpose of a radiological inventory

The radiological inventory of a nuclear waste is a quantitative description as accurate as possible of all the radionuclides it contains. Before the submission of the activity assessment

documentation (AAD) by the producer and its validation by ANDRA[1], the radiological inventory makes it possible to anticipate overall in a global manner the result of the method described in the future AAD for declaring the radionuclides in each package. It can best anticipate an *a priori* classification of the waste and develop management strategies that are best suited.

For the waste producer, knowing the radiological inventory of the graphite of UNGG reactors is essential above all for safety reasons related to the quality order of 10 August 1984 concerning the design, the construction and the operation of basic nuclear installations (BNIs). For decommissioning operations, knowledge of the radiological inventory allows the choice of the deconstruction tools and of the most suitable means of radiological protection to ensure staff safety. Moreover the identification of radionuclides behaviour in dismantling conditions that may lead to significant releases allows adapting the containment and purification barriers in order to limit the impact of these discharges on the environment.

Once the graphite is extracted from the reactors, the waste producer will produce an end package that will be an "important element for demonstrating safety" of the BNI that constitutes the ANDRA repository. Even in the absence of any particular specification on this package (everyone understands that it will depend on the disposal site which is not yet known), declaration of the radioactive content of the package at a minimum on the 144 radionuclides selected at the present time by ANDRA remains a prior essential factor in any shipment of the package to disposal.

As a "supplier" of an "important element for demonstrating safety of the ANDRA installation", the producer of the package is responsible for this declaration of activity on 144 radionuclides that will serve as a basis for the verification of conformity of the package with future specifications prior to their reception at ANDRA.

As long as the corresponding packages have not been accepted in the ANDRA BNI, the radiological inventory is not a fixed given established once for all and immutable over time. As is shown herein, it is the result of a rigorous procedure in accordance with the laws of physics. It is based on analytical results on samples taken in the reactor and on modelling seeking to mimic the phenomena explaining the presence of these radionuclides. Sometimes, in the

[1] French governmental agency in charge with nuclear waste management.

absence of a quantifiable element, reasoned choices are made for ensuring the over-assessment of the radiological inventory declared by the producer.

With improvements in analytical techniques and enrichment of accessible data through the implementation of new sampling campaigns and sample analysis, the radiological inventory of graphite may have to be specified for, while ensuring it is envelope, be as close as possible to reality.

5.2 Radionuclides in graphite

The radioactivity of the graphite in UNGG comes almost exclusively from the activation under neutron flux of the impurities and carbon 13 present in the material. The other radionuclides are naturally reactive radioelements such as potassium 40 impurities and the various isotopes of natural uranium.

In addition to the production of radionuclides by activation, it is also necessary, in a principle of completeness, to take into account a number of other phenomena which may also have affected the radiological inventory of the graphite during reactor operation:

- Radiolytic corrosion led to a mass loss of graphite by oxidizing some of the carbon atoms accessible to gases. These oxidized carbon atoms were released as CO_2 or CO in the cooling gas. During this erosion, some of the radionuclides present were able to be released into the cooling gas;
- Possible contamination of the graphite by the cooling gas, that was itself activated when flowing into the fuel channels of the graphite pile, would also have to be considered for generality purposes. However as will be shown later, the dispersion and the lack of any geographical correlation observed on measures of radionuclides in the graphite samples go against such phenomena of deposition of radionuclides. If these phenomena have existed, they were not significant in comparison with the activation phenomenon;
- Finally, in the particular case of the two fuel cartridges fusion accidents that have occurred in the reactors of the EDF Saint-Laurent power station in 1969 and 1980, the possible contamination of the graphite by fission products released into the cooling gas must also be considered. Moreover, it will be shown that, here again, nothing appears in the measurements of radionuclides that may be specific to such a contamination.

This section aims to describe in more detail the origin of the main radionuclides of interest in graphite as well as methods for their measurement. As it is not realistic in the context of the present document to describe the origin of all the 144 radionuclides with a half-life greater than 6 months that are requested by ANDRA in the context of safety studies for the long-term management of irradiated graphite, it has been chosen to focus on a few radionuclides considered representative of various phenomena that may occur in the reactor or considered significant for the management of graphite waste. These radionuclides of interest are the following:

- Major radionuclides in terms of activity in irradiated UNGG graphite, namely carbon 14 and nickel 63, example of long-life radionuclides, and tritium, a short-life radionuclide;
- Radionuclides considered being a sizing factor for storage of irradiated graphite with the example of chlorine 36, a radionuclide with a very long life. This radionuclide, although minor in terms of activity in irradiated graphite, is in fact mobile in a disposal situation, which makes it the first radionuclide released by the graphite disposal;
- Cobalt 60, a short-life radionuclide, which has been systematically measured in the analysed graphite samples. Cobalt 60 is in fact the main isotope contributing to the dose (γ tracer) used for sizing radiological protections. It is also easy to measure for the non-destructive quantitative measuring of waste packages or of waste basket just before packaging;
- Caesium 137, which is a product (γ tracer) of fission reactions of uranium. This radionuclide can attest to the presence or absence of fission products that may arise from uranium impurity in graphite or possibly from uranium of the fuel elements;
- Beryllium 10 and calcium 41, two radionuclides that are soluble in the underground water of the disposal repository and are the subject of particular attention for safety.

For more details on the origin of other radionuclides potentially or actually present in graphite, the reader can refer to reference [33]. The data concerning the radioactive characteristics of the

radionuclides described below are extracted from [34] and from [35] for the neutron cross sections.

5.2.1 Origin of some chosen radionuclides in graphite

Graphite is a synthetic material made from raw materials from oil and coal. Although subjected to extensive purification steps during the manufacturing process, some impurities remain in the nuclear graphite. Their content is very low and is of the order of a few grams of impurity per tonne of graphite (wppm: weight parts per million) and sometimes a few milligrams per tonne of graphite (wppb: weight parts per billion), which explains the strong heterogeneity observed experimentally of these impurities in trace amounts.

Tritium

Tritium is short-lived low energy radionuclide. It decays (half-life 12.33 years) by β^- emission to give rise to stable helium 3.

Tritium in the graphite of UNGG reactors can be produced through neutron activation of two impurities of the material:

- Boron activation according to ${}^{10}_{5}B+{}^{1}_{0}n \rightarrow 2{}^{4}_{2}He+{}^{3}_{1}H$, a reaction denoted ^{10}B(n,α)^{3}H with a mean effective cross section of thermal neutron capture $\sigma = 12 \cdot 10^{-3}$ barns;
- Lithium activation according to ${}^{6}_{3}Li+{}^{1}_{0}n \rightarrow {}^{4}_{2}He+{}^{3}_{1}H$, denoted ^{6}Li(n,α)^{3}H with a mean effective cross section of thermal neutron capture σ = 940 barns.

The concentrations of lithium and boron impurities in the graphite being equivalent and around 0.1 wppm, the tritium produced in UNGG graphite is almost exclusively due to the activation of lithium ^{6}Li(n,α)^{3}H, the neutron effective cross section of which is the highest.

Beryllium 10

Beryllium 10 is a long-life radioisotope of beryllium present in trace amount in the natural environment. Its radioactive half-life is 1 387 000 years. It is a pure β emitter that gives stable boron 10 by radioactive decay.

It can be produced in the reactor by neutron activation of beryllium 9 in accordance with the reaction ${}^{9}_{4}Be+{}^{1}_{0}n\rightarrow{}^{10}_{4}Be+\gamma$, denoted ^{9}Be(n,γ)^{10}Be with a mean effective cross section of capture of thermal neutrons of 0.0076 barns.

Carbon 14

Carbon 14 is a pure β emitter the half-life of which is 5 730 years and that give stable nitrogen 14 by radioactive decay.

There are three main ways for carbon 14 formation by neutron activation:

- Activation of the most abundant isotope of nitrogen (^{14}N) that is accompanied by the emission of a proton according to ${}^{14}_{7}N+{}^{1}_{0}n\rightarrow{}^{14}_{6}C+{}^{1}_{1}p$. This reaction is denoted ^{14}N(n,p)^{14}C;
- Activation of the isotope 13 of carbon, which leads to the emission of a γ photon according to ${}^{13}_{6}C+{}^{1}_{0}n\rightarrow{}^{14}_{6}C+\gamma$, a reaction denoted ^{13}C(n,γ)^{14}C;
- Activation of the isotope 17 of oxygen, which is transformed into ^{14}C with the emission of a helium nucleus (α) according to ${}^{17}_{8}O+{}^{1}_{0}n\rightarrow{}^{14}_{6}C+{}^{4}_{2}He$ and denoted ^{17}O(n,α)^{14}C.

These reactions are listed in Table 16 with, for each of them, the capture cross section as well as the natural abundance of the various isotopes giving rise to the production of carbon 14.

Table 16. Main routes of carbon 14 generation in nuclear graphite [35]

Pathway	Thermal neutrons capture cross section in barns (10^{-24} cm^2)	Abundance of isotope in natural element (%)
^{14}N(n,p)^{14}C	1.91	99.63 ^{14}N / nitrogen
^{13}C(n,γ)^{14}C	0.00137	1.07 ^{13}C / carbon
^{17}O(n,α)^{14}C	0.236	0.04 ^{17}O / oxygen

In case there would be equivalent amounts of nitrogen, carbon and oxygen, by far the most favourable route to produce carbon 14 would be the activation of nitrogen. However, nitrogen is present in the graphite as trace amount and potentially provided by the cooling gas (values less than 1 %). Due to the massive presence of carbon in the graphite core, activation calculations actually show a balance between ^{14}N(n,p)^{14}C and ^{13}C(n,γ)^{14}C reactions for the production of carbon 14 within the graphite matrix (see Table 17). In the cooling gas,

carbon 14 is essentially produced by reactions $^{14}N(n,p)^{14}C$ and $^{17}O(n,\alpha)^{14}C$ with oxygen supplied in the form of CO2 and CO that are impurities of the cooling gas [36].

The distribution of the carbon 14 in graphite between the reactions $^{14}N(n,p)^{14}C$ and $^{13}C(n,\gamma)^{14}C$ highly depends on the nitrogen content in the graphite reactor operating conditions. It can by show by activation calculations [37] that, in the case of UNGG reactors, when the nitrogen content in the graphite is assumed to be 4 wppm, 70 % of the carbon 14 is formed by reaction $^{13}C(n,\gamma)^{14}C$. When this nitrogen content increases to 51 wppm in the graphite, the carbon 14 is then produced by reaction $^{14}N(n,p)^{14}C$, to the extent of 83 %.

Table 17. Calculated ^{14}C production (neutron activation only) in CO_2-cooled reactors [38]

Origin	Production rate (TBq / GWe·year)		Main pathway
	MAGNOX	AGR	
Cooling gas	$2\ 10^{-3}$	$2\ 10^{-3}$	$^{13}C(n,\gamma)^{14}C$
	0.27	0.26	$^{14}N(n,p)^{14}C$
	0.04	0.04	$^{17}O(n,\alpha)^{14}C$
Nuclear fuel	$3\ 10^{-5}$	$7\ 10^{-6}$	$^{13}C(n,\gamma)^{14}C$
	4.8	0.48	$^{14}N(n,p)^{14}C$
	$4\ 10^{-4}$	0.12	$^{17}O(n,\alpha)^{14}C$
Graphite moderator	4.1	1.3	$^{13}C(n,\gamma)^{14}C$
	6.7	2.2	$^{14}N(n,p)^{14}C$
	$7\ 10^{-4}$	$3\ 10^{-5}$	$^{17}O(n,\alpha)^{14}C$
Total	15.9	4.4	

Compared with reactors similar to UNGG reactors (graphite moderated and CO_2 cooled), it is shown in the literature that the main part of the production of ^{14}C in graphite arises from these two reactions. Most publications that refer to this subject uses the results of a single study published in 1983 [38], which explains that, in the cooling gas and in the fuel, ^{14}C is mainly produced from nitrogen, while in the moderator (that is to say the graphite), there would be some rebalancing between the two reactions $^{14}N(n,p)^{14}C$ and $^{13}C(n,\gamma)^{14}C$ (see Table 17).

However, the results presented in Table 17 do have to be carefully interpreted. They depend on the operating characteristics of the various reactors and the impurities that are associated therewith, especially nitrogen. The publication in which these results are presented itself refers to other older publications not accessible; it has therefore not been possible to verify the assumptions and calculations taken into account and in particular the evidence for the nitrogen content in the graphite and in the cooling gas.

Chlorine 36

Chlorine 36 is a radioactive isotope of chlorine present in trace amount in nature. This is mainly a β emitter with a half-life of 301 000 years that by β^- disintegration gives stable argon 36.

It may be produced in nuclear reactors in various ways. The only two direct formation routes by activation in graphite are:

- Production from the stable isotope 35 of chlorine[2] according to the reaction ${}^{35}_{17}Cl + {}^{1}_{0}n \rightarrow {}^{36}_{17}Cl + \gamma$, denoted ^{35}Cl(n,γ)^{36}Cl with a mean effective cross section of capture of thermal neutrons σ = 44.1 barns;
- Production from the stable isotope 39 of potassium[3] according to the reaction ${}^{39}_{19}K + {}^{1}_{0}n \rightarrow {}^{36}_{17}Cl + {}^{4}_{2}He$, denoted ^{39}K(n,α)^{36}Cl with a mean effective cross section of capture of thermal neutrons σ = 2 barns.

It may also be formed indirectly. The main indirect pathway is the neutron activation of the stable isotope 34 of sulphur[4] which gives rise to the β emitter isotope 35 of sulphur, which then leads to the stable isotope 35 of chlorine, the precursor of chlorine 36 by neutron activation ${}^{34}_{16}S + {}^{1}_{0}n \rightarrow {}^{35}_{16}S$, then ${}^{35}_{16}S \rightarrow {}^{35}_{17}Cl + {}^{0}_{-1}e$.

The relative importance of each of these reactions for the production of chlorine 36, normalised with respect to the reaction of formation from natural chlorine, was calculated in the case of the neutron flux received by graphite sleeves of MAGNOX reactors [39]. It is $8.5 \cdot 10^{-4}$ for potassium and $3.2 \cdot 10^{-5}$ for sulphur, which would mean that an initial concentration of each of these elements of respectively 1 200 times greater than that of natural chlorine in the case of potassium and 31 000 times greater for sulphur would be needed so that the production of chlorine 36 from these two elements becomes actually significant. The analysis of a non-irradiated graphite sample from Saint-Laurent A2 pile reveals potassium concentrations below 2 wppm (g/t) and sulphur of around 30 wppm for a chlorine content of 8 wppm. Other data

[2] Isotope abundance 75.77 %.

[3] Isotope abundance 93.26 %.

[4] Isotope abundance 4.21 %.

confirm that the sulphur or potassium contents are of the same order of magnitude as that of chlorine or up to one order of magnitude higher. With these levels of sulphur and potassium impurities, it appears that the reaction ^{35}Cl(n,γ)^{36}Cl is the by far the predominant reaction for the formation of chlorine 36 within graphite.

Calcium 41

Calcium 41 is a long-life radioisotope of calcium the radioactive half-life of which is 102 000 years. It gives stable potassium 41 by β^+ emission.

It can be produced in the reactor by neutron activation of the isotope 40 of calcium[5] according to the reaction ${}^{40}_{20}Ca + {}^{1}_{0}n \rightarrow {}^{41}_{20}Ca + \gamma$, denoted ^{40}Ca(n,γ)^{41} with a mean effective cross section of capture of thermal neutrons of 0.41 barns.

The fact that such a radionuclide comes to man only by dissolution in water which will be oversaturated with stable natural calcium because of the huge quantity of concrete of the repository should be taken into account.

Cobalt 60

Cobalt 60 is a radioisotope of cobalt the radioactive half-life of which is 5.3 years. It gives stable nickel 60 by β^- disintegration with the emission of two γ lines (826 and 1 332 keV). This radioisotope is widely used in industry and radiotherapy.

It can be produced in the reactor by neutron activation of cobalt 59 (the only natural isotope of cobalt) according to the reaction ${}^{59}_{27}Co + {}^{1}_{0}n \rightarrow {}^{60}_{27}Co + \gamma$, denoted ^{59}Co(n,γ)^{60}Co with a mean effective cross section of capture of thermal neutrons of 37.18 barns. Cobalt is an impurity of nuclear graphite to the extent of approximately 1 gram of cobalt per tonne of graphite (1 wppm, which is usually a detection limit) or even much less [37]. One assumption that is sometimes suggested is that it could also be brought in contact with the graphite by the deposition of corrosion products coming from metal components (ferritic steels) internal to the reactor. Such an assumption would be confirmed only with the proof of a geographical auto-correlation of ^{60}Co measurements, which is not the case in EDF graphite.

[5] Isotope abundance 96.9 %.

Nickel 63

Nickel 63 is a low-energy pure β emitter the half-life of which is 101.2 years. By β^- disintegration, it gives rise to stable copper 63.

It is produced by neutron activation of the isotope 62 of nickel[6] according to the reaction ${}^{62}_{28}Ni + {}^{1}_{0}n \rightarrow {}^{63}_{28}Ni + \gamma$, denoted ^{59}Co(n,γ)^{60}Co with a mean effective cross section of capture of thermal neutrons of 14.5 barns.

Caesium 137

Caesium is a radioactive element with a half-life of 30.8 years. It gives metastable ^{137m}Ba by β^- emission with a very short life, and which gives stable ^{137}Ba with γ emission (661 keV).

Unlike the previous radionuclides (and unlike caesium 134), caesium 137 is not an activation product. It is one of the fission products of uranium. In this regard, it's possible presence in UNGG graphite may testify to a contamination of the graphite by the fission products of the uranium in the nuclear fuel (rupture of fuel assembly cladding) but, as will be shown below, it comes mainly from the fission of traces of uranium initially present in the graphite.

5.2.2 The measurement of radionuclides in the graphite

As recommended in [33] for the assessment of a radiological inventory "the result of any theoretical calculations should be compared with the data obtained by experiments to obtain a validation of the calculations". This section is devoted to the description of the work done on graphite samples from EDF UNGG reactors in order to obtain reliable data used for the radiological inventory.

Graphite sampling

Measurement of radionuclides in the irradiated graphite passes through sampling. It is done by core sampling operations that are time consuming, complex and costly, using various techniques. For CEA reactors G1, G2 and G3 at Marcoule, the core samplings were carried out directly through the concrete vessel of the reactors into the graphite pile. The diameter of the tool used for drilling was around 63 mm. For EDF reactors, remote-control tools introduced into the fuel channels of the piles were used. This technique is the same to the technique implemented for monitoring the wear of the graphite during operation. The remote-control tool

[6] Isotope abundance 3.6 %.

(see Fig. 11) was introduced from accesses through the refuelling pits at the upper part of the reactor into the channels, and performed coring on either side of the graphite bricks in the direction perpendicular to the channels with a hole diameter of about 20 mm.

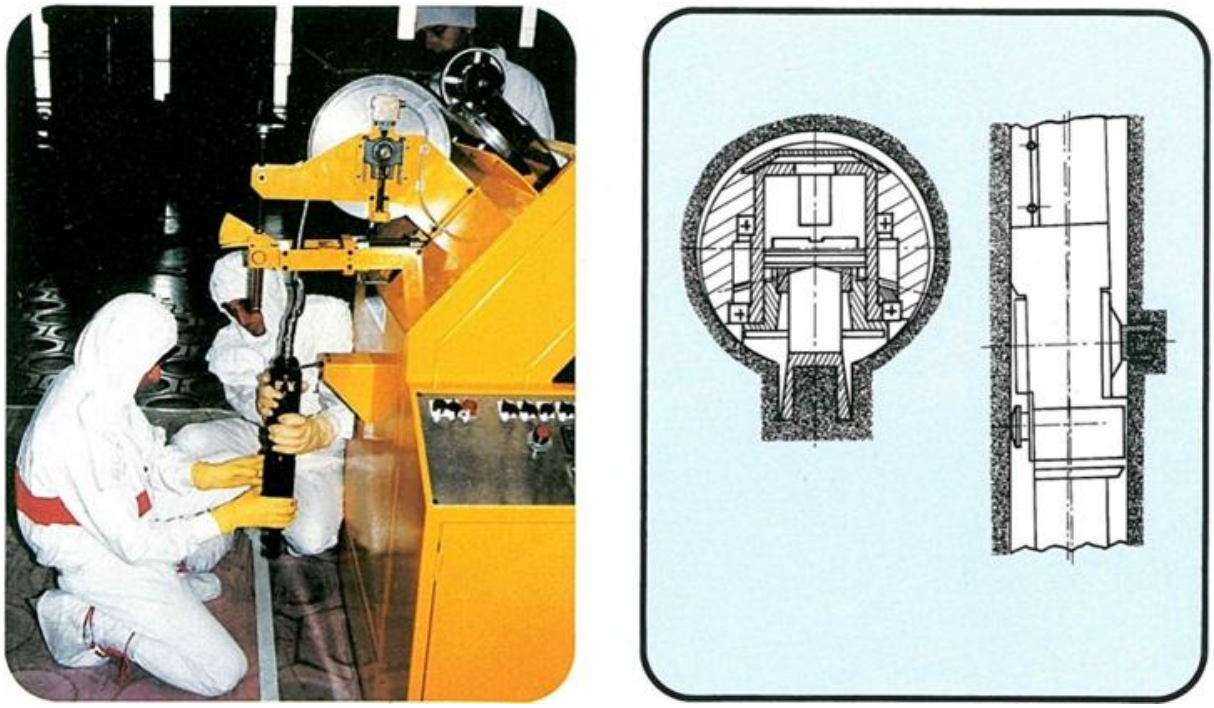

Fig. 11. Remote-control tool used for the sampling of graphite core from EDF's UNGG reactors [40]

The cylindrical graphite carrots sampled therefore have a variable size depending on the tools. Their weight can range from about 20 grams up to 650 grams as shown in Fig. 12.

Fig. 12. Graphite samples from CEA G2 reactor (left) and EDF Saint-Laurent A2 reactor (right)

Samples are chosen in order to have an available panel of samples from different areas distributed over the entire height and circumference of the pile. This ensures to get representative samples of the variability of operating conditions encountered in the reactor in

terms of temperature and neutron flux in particular. For EDF reactors, depending on the dimensions and geometry of the cores, a set of 20 to 30 irradiated graphite carrots is generally analysed by radiochemistry out of the 200 carrots taken on average per reactor.

Reproducibility of analyses but high sampling variance

Most of radiochemical analyses of graphite samples were performed by CEA LARC in Cadarache according to various techniques described in CARBOWASTE project Deliverable D-3.3.1 [41].

Reproducibility is the closeness of the agreement between the results of successive measurements (replicas) of the same homogenate by varying the measurement conditions. It is also expressed by the standard deviations of the fluctuations of the signal for the measurement of which at least one of the operating parameters is modified, for example with different operators or different test samplings.

The reproducibility of the analyses was verified experimentally (i.e. coherently with measurement uncertainty) by comparing successive measures obtained on several samples coming from the same aliquot (same sample of a shredded carrot). For the main radionuclides concerned, this reproducibility was also attested for different activity levels. The curves presented in Fig. 13 illustrate the reproducibility of the results obtained in the case of carbon 14 for two different activity levels.

In the case of the radionuclides present in very small quantities such as chlorine 36, the reproducibility of the results is much more difficult to achieve especially when different samples from the same aliquot are used as shown in Fig. 14.

The fundamental physical phenomenon that explains this difficulty in the reproducibility of the analyses for the elements present in trace amount has nothing to do with the quality of the sampling. The performance of the measuring laboratory is also not at all in question. It is a case of the variance that affects the measurement of a sample for representing a concentration (chemical content or specific activity) of a given batch, according, among other parameters, to the concentration, the mass of the sample or the mass of the batch. This phenomenon, which it will be attempted to explain briefly below, was in particular theorised by Pierre Gy and readers wishing for further information can refer to reference [42].

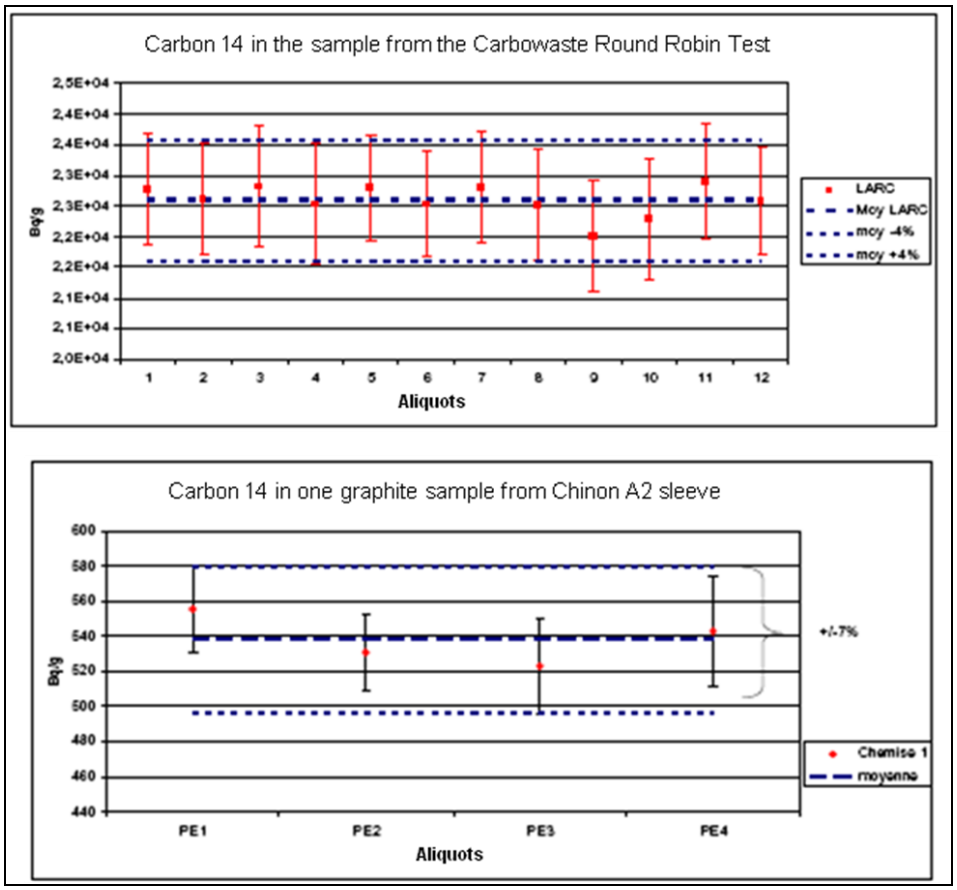

Fig. 13. Reproducibility of radionuclide measurements in graphite samples: the carbon 14 (by courtesy of J. COMTE CEA LARC)

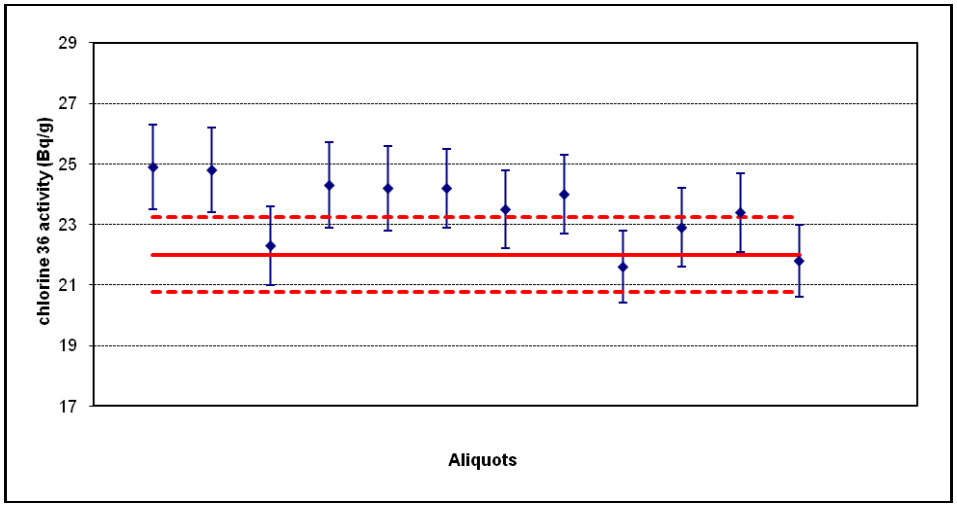

Fig. 14. Reproducibility of radionuclide measurements in graphite samples: chlorine 36 (by courtesy of J. COMTE CEA LARC). In blue – measurements with their uncertainties, red line – defined value of the tested sample with its uncertainty (dotted lines)

If a sample of mass M_e is taken, normally low in relation to the mass M_L of the batch from which it is extracted, the relative variance of the fundamental sampling error can be written, by grouping together in a factor K the other parameters of influence, as a particular expression of the Gy formula (4):

$$\frac{s^2}{a_L^2} = s_r^2 = \frac{1-a_L}{a_L}\left(\frac{1}{M_e} - \frac{1}{M_L}\right)K\,; \qquad (4)$$

where

M_e – the mass of the sample is given in grams;
M_L – the mass of the samples batch is normally much greater than M_e;
a_L – the concentration of the component of interest expressed in the form of a weight fraction.

In the case of graphite samples, the mass of the sample is negligible compared with the mass of the batch since it is equal to approximately half a gram for the measurement.

The characteristic of the impurities of nuclear graphite is their very low proportion, for reasons that are fully understandable related to the neutron performances necessary for obtaining criticality despite the use of "non-enriched" uranium (UNGG).

From these two findings the following simplified formula (5) comes:

$$s_r^2 \approx \frac{1-a_L}{a_L}\frac{K}{M_e} \approx \frac{K}{a_L M_e}\,. \qquad (5)$$

The Gy formula was essentially originally elaborated from the hypergeometric discrete distribution law that describes the probability of drawing "*m*" white balls ("*m*" fragments of chlorine to give an idea on a practical example, chlorine being the species of interest, the concentration of which is sought) from "*n*" ("*n*" fragments of the carbon + chlorine mixture) when the complete batch contains "*M*" white balls (chlorine) among "*N*" balls (the chlorine + carbon mixture) in a drawing without putting back in order to model the taking of a sample (of "*n*" fragments of the mixture).

This hypergeometric law, when N is large[7], can be approximated by a binomial law and, with the notation $p = M/N$ for the concentration of the batch (here the pile), the expectation and the

[7] 100 Bq of chlorine 36 per g of graphite corresponds referred to an atomic scale to a ratio of 1 atom of chlorine 36

variance of the random variable *m/n* can be calculated, which corresponds to the (chlorine) concentration measured.

Let us use the fact that the law is very close to the binomial law, which makes it possible to write its mathematical expectation:

$$E(m/n) = p\ ; \tag{6}$$

and its variance:

$$[\sigma(m)]^2 = np(1-p) \Rightarrow \left[\sigma\left(\frac{m}{n}\right)\right]^2 = \frac{p(1-p)}{n}. \tag{7}$$

The relative variance is a dimensionless quantity since it is the square of *σ(m/n)/E(m/n)*. The relative variance of this measured concentration will therefore be written as:

$$[\sigma(m/n)/E(m/n)]^2 = \frac{(1-p)}{np}. \tag{8}$$

This formula indicates that the concentration "*p*" of the batch (the pile) and the number of fragments "*n*" in the sample (the sampling) each fulfil an essential role in the relative sampling variance. The fundamental relative variance of the sampling therefore increases when the number "*n*" decreases and/or when the number "*p*" decreases; thus the lower the concentration the higher the relative variance increases. Likewise, the more the number of fragments in the sample decreases, the more the relative variance increases. However, the number of fragments is directly proportional to the mass of the sample.

The relative variance of the measurements of the content on sampling, corresponding to the fundamental relative sampling variance, is therefore inversely proportional to the mass of the sample (corresponding to the number "*n*" of fragments of the sample) and/or to the true content (corresponding to "*p*", the true chlorine 36 concentration of our example) when this is low.

The formula (5) given previously is indeed found again – $s_r^2 \approx \frac{1-a_L}{a_L}\frac{K}{M_e} \approx \frac{K}{a_L M_e}$. This formula explains the relative variance of a sample for representing the content of a given batch (here the graphite pile) according to the mass of the sample (corresponding to the mass of the

for $36 \cdot 10^6$ atoms of carbon, assuming as a first approximation that the graphite consists solely of carbon atoms.

sampling of less than 1 gram) and the content of the constituent of interest (for example chlorine 36 and/or chlorine).

Variability of measurements

There sometimes is a very large variability between different homogenates from the same shredded carrot. This variability in a centimetric scale is particularly marked in the case of chlorine 36 measurements. It is illustrated in Table 18, which, for different homogenates coming from the same graphite carrot, reproduces the results of chlorine 36 measurements. This Table 18 presents the measurement (at least two samplings per measurement) obtained on the homogenates prepared separately from the ends 1 and 2 and the middle part cut from the same carrot (see Fig. 15). These values are compared with the measurement made on the powder collected during the cutting of the various parts (called "powder from the cutting" in the Table 18).

This centimetric-scale variability was confirmed on several carrots coming from different reactors. It is intrinsic to the heterogeneity of the material observed by microscopic techniques. Chlorine appears in the form of a heap of micrometric size.

The heterogeneity observed on the impurities repartition leads logically to the heterogeneous repartition of the radionuclides. To be simple, the activity of the radionuclide is the product of the flux that varies continuously by a factor of less than 10 over several metres of a graphite pile, by the concentration of the impurity that varies randomly by a factor greater than 10 or even 100 over distances as low as a centimetre in the graphite pile.

Table 18. Chlorine 36 measurements (in Bq/g) from different parts of one same graphite sample (by courtesy of J. COMTE CEA LARC)

Location	G2-27	G2-32	G2-42	G2-46
end 1	230±27	190±25	698±81	7±1
middle	180±24	123±14	135±17	115±17
end 2	256±30	211±24	1316±147	15±2
Mean value	222±40	174±46	716±516	45±60
Powder from cutting	180±24	149±16	225±35	108±19

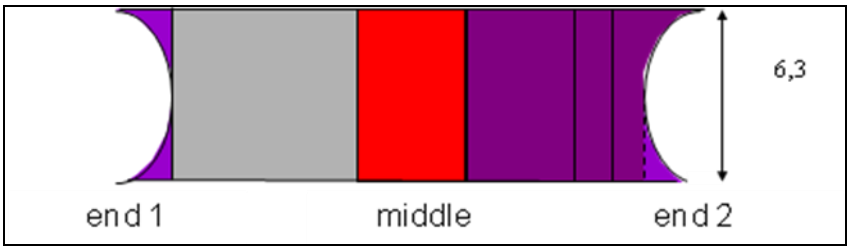

Fig. 15. Cutting plan of a graphite sample (by courtesy of J. COMTE CEA LARC)

At the scale of the pile, this variability over sometimes two orders of magnitude is also observable. Fig. 16 presents by way of example the distribution of the chlorine 36 measurements obtained on graphite samples taken from graphite cores in the EDF reactors at Chinon A3, Saint-Laurent A1 & A2 and Bugey 1.

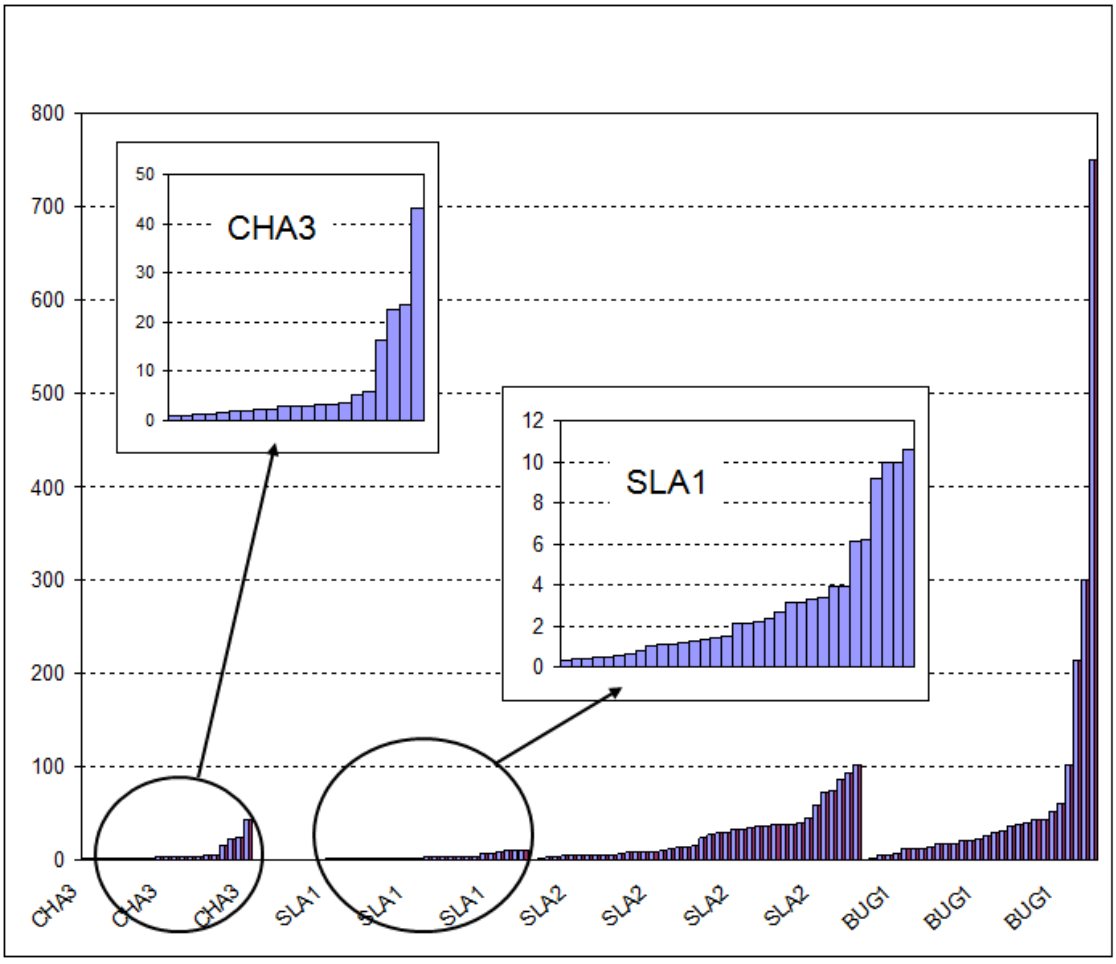

Fig. 16. Chlorine 36 measurements (in Bq/g) on graphite sample from EDF UNGG reactors – CHA3 stands for Chinon A3, SLA for Saint-Laurent and BUG1 for Bugey 1 reactors

This very high variability observed at the scale of a pile cannot be explained by the variability of the neutron flux, giving rise to the production of chlorine 36, which is not as great (in the graphite moderator the mean transport length of the neutrons is around 60 cm). Fig. 17 shows the dispersion of the measurements of chlorine 36 in the samples from the Bugey 1 reactor according to their sampling position in the graphite pile[8]. The variability of these measurements is correlated neither with the variation of the neutron flux according to the altitude (see Fig. 18), nor with the other macroscopic operation parameters of the reactor, such as the temperature, which varies at full power approximately linearly from 280 °C to 530 °C between the top of the pile and the bottom during the Bugey 1 operation (cooling gas circulation from top to bottom in integrated-vessel reactors such as Bugey 1, Saint-Laurent A1 & A2).

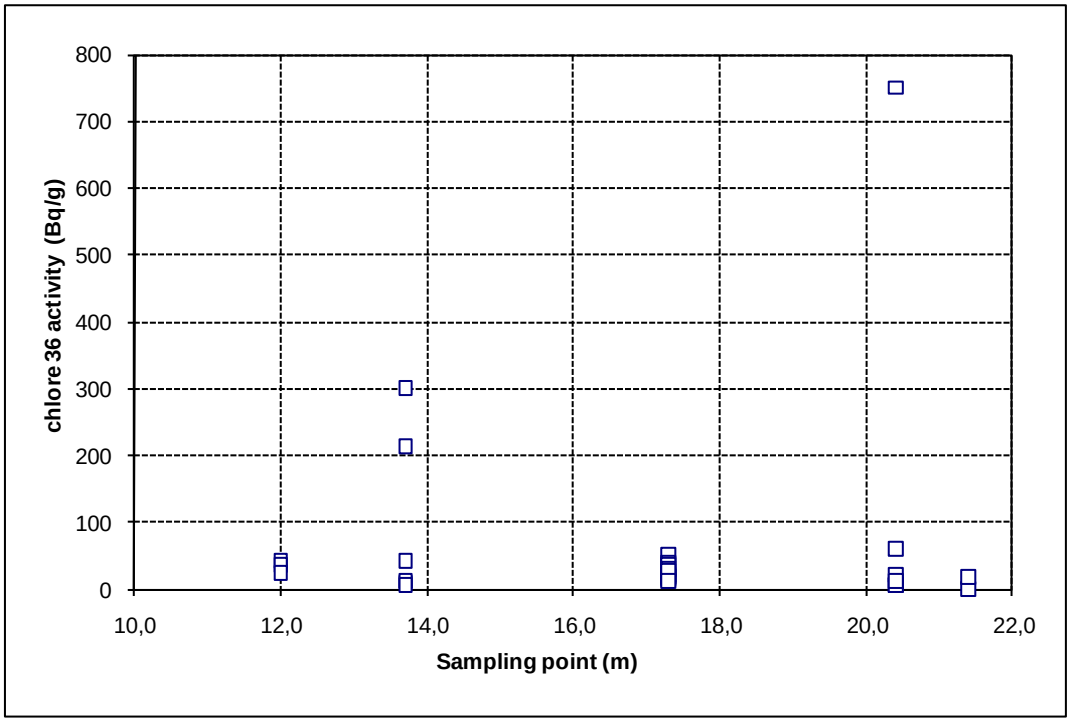

Fig. 17. Chlorine 36 measurements (in Bq/g) in samples from Bugey 1 pile: x-axis – height of the sampling point in the pile

This high variability of the measurements shows that it is not possible to obtain measurements of radionuclides present in small amounts such as chlorine 36, representative of an object at the scale of a graphite brick and even less at the scale of an entire pile. This observation has led

[8] For Bugey 1, the heights are given with reference to the top cap of the reactor vessel in metres. The Bugey 1 graphite pile consists of 12 beds of graphite bricks. The bottom of the pile (bed n_o 1) is at 21.80 m with respect to the level of the top cap, while the top of the pile (bed n_o°12) is at 11.60 m.

EDF to provide for the establishment of the radiological inventory of graphite piles, an approach based on a statistical approach by calculating an average of several measurements. The average is the only method that allows dividing the variance by the number of measurements to be reliable, whereas extreme values (minima and maxima) may by definition represent singular measures very far from the average reality. This approach is detailed in the following section devoted to inventory modelling.

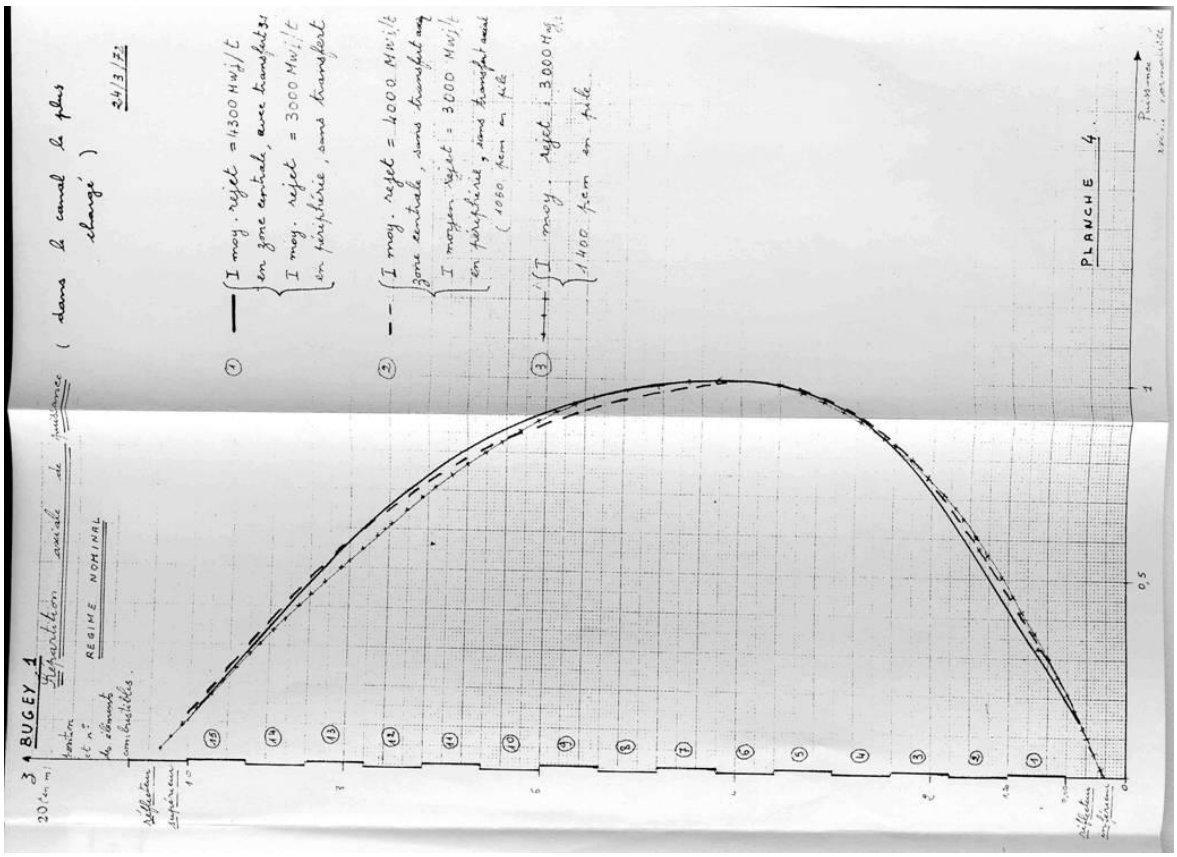

Fig. 18. Shape of the thermal power (correlated to the neutron flux) in a fuel channel of the Bugey 1 reactor: x-axis – height of the pile; y-axis – full power in arbitrary units

5.3 Assessment of the radiological inventory of EDF graphite

5.3.1 Drawbacks of an inventory model based on a measurement of maximum activity

As previously illustrated, the high variability observed on the measures of the various radionuclides shows that taking into account a single measurement (for example the maximum recorded value as chosen in the French preliminary inventory made by ANDRA in 2007) can

lead to a significant overestimation of the radiological inventory when aligning the graphite activity at any point of the pile on this value. This overestimation is particularly damaging in the case of sizing radionuclides such as chlorine 36, which is present in the trace amounts, as shown above, and exhibits a very high dispersion of its measures.

Moreover, taking as a reference only one measuring point does not make it possible to link the finding made (the measurement) with the physical phenomena giving rise to the radionuclides and in particular with the first of them, the activation of the impurities by the neutron flux in the reactor. This lack of correlation between the measures and the phenomenon at the origin of radionuclides (neutron activation) raises the crucial problem of the representativeness of this single measurement. Only the use of a set of measurements and their mean value is a real guarantee of representativeness.

5.3.2 Why is a conventional activation calculation not possible?

We will call "conventional activation calculation", a calculation of the radionuclides formed by activation of a supposed known amount of impurities giving rise to these radionuclides. These are therefore postulated impurities since no preliminary process is used to estimate them from the measurements and the activation calculations. Although it is conventional in the literature to use this approach, it turns out to be totally unsuitable in the case of the graphite in the EDF UNGG reactors for at least two reasons discussed in more detail in the following:

- This approach requires knowing the impurity content at the origin of the radionuclides. This data is very often difficult to know accurately, and is sometimes missing for various reasons;
- The graphite in a reactor undergoes complex physicochemical phenomena that can lead to the release into the cooling gas of some radionuclides produced in the graphite. Thus, the radiological inventory of the UNGG graphite is the result of phenomena that lead to the production of radionuclides (neutron activation), and of phenomena leading to elimination of part of their stable precursors or part of them from the graphite (thermal release, radiolytic corrosion, etc.). It is not possible to take into account these phenomena through a conventional activation calculation.

The lack of data on the impurity levels

The identification and the measurement of pristine impurities in the graphite and liable to have been activated during operation is not a trivial problem. The issue of the impurities which can have an impact on the management of the future nuclear waste was not always considered at the time of the construction of the reactors. The graphite from the various manufacturing plants was indeed always characterized from the viewpoint of its moderating properties (measurement of the capture cross sections in CEA experimental reactors) and of its physical properties that determined its mechanical properties (density). But, most of time, it was not characterized from the viewpoint of the totality of its chemical composition. The chemical composition of the nuclear graphite and the analysis of its impurity content have not been determined for all the impurities of interest. Even if there are many data available on this issue in the archives of the CEA and EDF, however, they are far from being exhaustive.

In addition, another important point that should be emphasised concerns the very low impurity content which led in the past and without exception indeed, to operational difficulties to measure them with the required accuracy. Whereas for the radioactive elements, it is relatively easy to achieve detection limits of the order of the Bq/g, which in terms of mass is of the order of a few milligrams per tonne of graphite (wppb), for the elements that produce no radiation, their detection by conventional chemical methods is often limited to levels of the order of one milligram per kilogram of graphite (wppm).

Moreover, beyond these technical difficulties, the case of nitrogen, one of the precursors of carbon 14, is an example of an impurity which is a real impossibility to determine its content in the graphite under operating conditions. The nitrogen can be present in virgin graphite as an impurity introduced by the raw materials used for its manufacture (including air trapped in the closed pore structure), but it could also have been added or removed during the operating period. The adsorption of nitrogen on the surface of the graphite is a well known phenomenon, and nitrogen is an impurity in the coolant gas that can also come from an air inlet voluntary (maintenance periods) or involuntary (leaks), into the atmosphere of the reactor. Its measurement in the graphite moreover constitutes a real challenge, since it is very difficult from the operational viewpoint to avoid the pollution of the graphite by the nitrogen from the air during the implementation of this measure.

Studies performed on nuclear graphite have assessed the capacity for nitrogen adsorption at the surface of nuclear graphite at values between 40 and 150 wppm [43] for temperatures up to 400 °C. However this kind of measurement has always been performed on non-irradiated graphite in conditions (under air or nitrogen) that are very far from the usual operating conditions in a nuclear reactor. Under irradiation with carbon dioxide, it is well known that the carbon surface of the graphite is continuously oxidised: this very certainly leading to the release of a significant part of the nitrogen that could have been adsorbed on it.

Although a "mean" nitrogen content of 50 wppm is sometimes used in certain publications [36] in order to estimate the ^{14}C inventory by activation calculation, application of such data to the case of the graphite in the UNGG reactors of EDF leads to calculated carbon 14 contents that are greater, by at least 1 order of magnitude, than those actually measured. In addition, certain published measurements on the graphite of UNGG reactors before use in the reactor detected nitrogen levels of the order of 4 wppm [33], which seem to be more compatible with the carbon 14 activity levels actually measured on irradiated graphite.

The phenomenon of radionuclide release in a reactor

Another phenomenon that makes the determination of an inventory of the irradiated graphite by conventional activation calculation a very hazardous operation is the release of the radionuclides and/or of their stable precursors that occurs in the reactor with temperature and irradiation. The conventional calculation by activation of a postulated impurity does not account for this phenomenon of the potential release of radionuclides by the graphite. This release had indeed been demonstrated in the case of chlorine for the graphite of British reactors for example. Chlorine 36 has thus been observed in samples taken in the cold parts (into the dryer of the cooling gas) of MAGNOX reactors [44].

Moreover there are reasons to believe that with the radiolytic corrosion that can lead to losses of graphite mass close to 40 % in some parts of the pile of some reactors, a significant part of the radionuclides formed by activation of the material could be released back into the cooling gas of the operating reactor. Since the spatial and temporal distribution of the release in general (of the stable precursor or of the radionuclide), and of the radiolytic corrosion in particular, almost completely escapes the realm current knowledge, the usual method based on a postulated impurity, is therefore particularly unsuitable for answer the question of the radiological inventory of irradiated graphite.

5.3.3 Principle of the identification calculation-measurement method

The general case of the piles

EDF has chosen to develop a method of 3D geographical reconstitution of the inventory of the nuclear piles that is based on an activation calculation which is adjusted by minimisation of a standard deviation of the calculation result with a mean value of the several measurements available. The objective of developing this method is twofold. By using a statistical approach to the measurements, and not an approach based on the maximum measurement, the measured data is made more representative. Apart from this, the use of an activation calculation results is a closer approach to the reality of the main phenomena at the origin of radionuclides in a reactor, while also incorporating the secondary effects that can alter this result (release during the operation of the reactor). In order to be able to take account of these possible secondary effects, this calculation is performed without prejudging any initial impurity content, or the behaviour of this impurity in operating conditions. The impurity content is determined by prior calculation of its best estimate. It is based upon measurement of the levels of radioactive elements (radionuclides), which are much easier to detect than the non-radioactive impurities, for the very small quantities observed in the nuclear graphite, since the radioactivity is then the only magnitude that is measurable. This enables to compute an explanatory impurity content from the measurements performed on samples by reverse activation calculation.

The method of inventory assessment by identification calculation-measurement [45] consists of using the following process (shown in the simplified diagram in Fig. 19), so as:

- In a first step, to calculate a 3D map of the flow of neutrons of different energy levels in the reactor pile concerned in the calculation. This map is created by the CEA, based on the geometry of each pile, with the TRIPOLI calculation code, which is a code for the transmission of particles (neutrons) solving the Boltzmann equations, coupled with nuclear databases (ENDF, JEF-2);
- In a second step, from this map of the flux, and incorporating the history of reactor operation, to reconstruct a global inventory of the radioactivity produced by this flux throughout the geometry of the reactor pile. The inventory is then created by incorporating the impurity levels, which are adjusted to their explanatory values by a method of least squares, from the result of the activation calculation with the available

measurements of the corresponding radionuclides. These activation calculations are performed by EDF, using the DARWIN/PEPIN code which is used to integrate all of the phenomena that lead to the production of radionuclides (activation, fission, radioactive decay, etc.) by solving the Bateman equations;

- In a third step, use is made of the fact that each radionuclide measurement is characterised by a specific standard deviation that is dependent on the number of measurement points available. This standard deviation, which is individual to each radionuclide measurement, is used to calculate a confidence interval for its mean calculated value. For an overall determination of the inventory, we consider the upper value of the confidence interval (which corresponds to a 2.5 % risk of under-evaluating the result) of the ratio in relation to the cobalt 60 gamma tracer, in order to remain consistent with the choices made conventionally by ANDRA;
- In a fourth step, in order to determine the value of activity to be declared for each radionuclide, we consider the upper value of the confidence interval of the cobalt 60 tracer, which thus corresponds to a mass-related activity to which is added a 2.5 % risk of under evaluation, and we multiply this upper value by the upper value of the ratio previously calculated for the radionuclide concerned.

The relevance of the method for inventory calculation by adjustment calculation-measurement is based upon the availability of a sufficient number of measurements of the wanted radionuclides carried out on samples of irradiated graphite. These data, in sufficient number, are processed using the Central Limit Theorem (CLT), which is employed in order to determine the uncertainty in the activity measured (which is a Gaussian curve by application of the CLT).

The acquisition of measurements is a long and costly process that should have been optimised. Since the variance of a mean is obtained by dividing the variance of the population of measurement points by the number of points, then the larger this number of measurement points the greater the standard deviation and the smaller the confidence interval on the mean value of the activity of a given radionuclide. This is used to directly obtain the uncertainty calculated from:

- Statistical measurement data and the associated adjusted calculations;
- The number of points used; and
- The under-assessment risk selected.

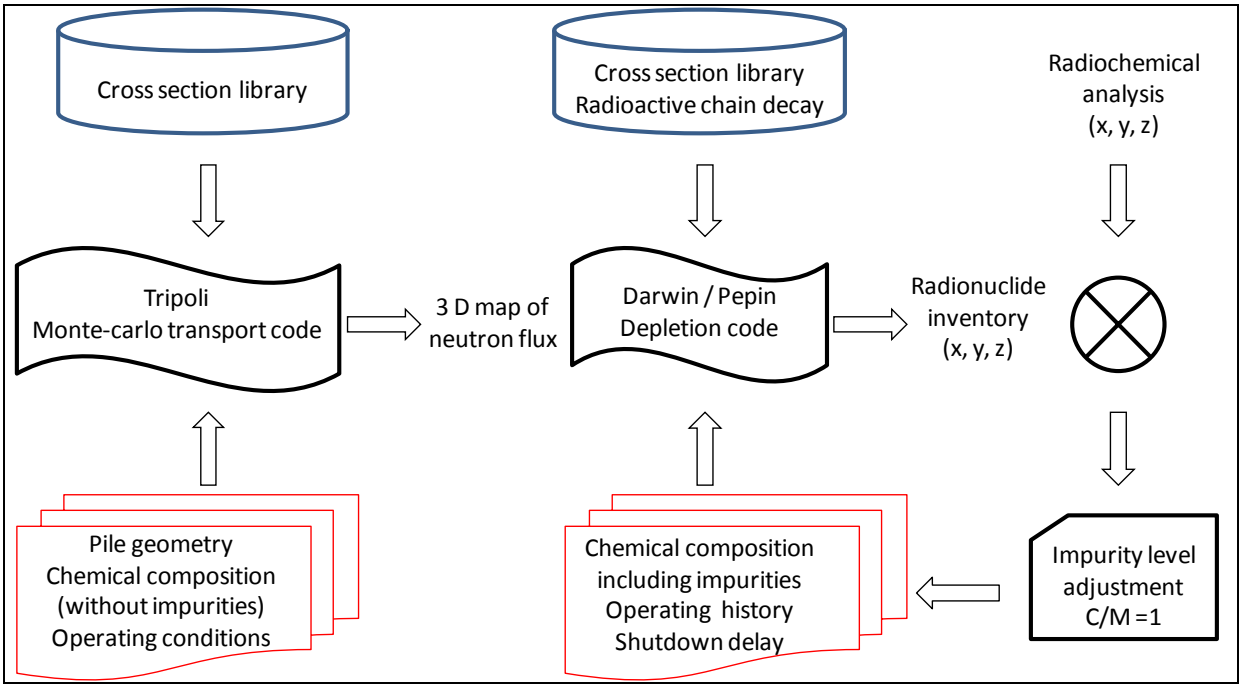

Fig. 19. Simplified description illustrating the general principles adopted for calculating the radiological inventory of piles in the EDF reactors by identification calculation-measurement

In practice, for each reactor, EDF has arranged for the analysis of some thirty radionuclides on some thirty samples of graphite taken from the reactor. It is from an order of magnitude of about 30 points that the number of points can be seen as always being sufficient since the withdrawal of any of these does not significantly change neither the estimate of the mean nor its confidence interval. On the other hand, below 15 points, the calculation that employs the Student Law introduces a penalty in terms of increasing the size of the confidence interval.

Generally, by taking account of the measurements below the detection limit, about 900 measured, of which about 350 were at the detection limit, have been included for each reactor, for the cores of the Saint-Laurent A1 & A2, Chinon A3 and Bugey 1 reactors.

The support areas processed like the piles

For the integrated vessel reactors (Saint-Laurent A1 & A2 and Bugey 1), graphite billets have been used as biological protection in the support area of the pile. This graphite, which is intended to prevent activation of the lower metal structures (heat exchangers) by the residual radiation coming from the pile, has itself been poorly activated by this residual flux.

For this reason, the radiological inventory of the latter has also been calculated. Since this is the same graphite as that which was sampled from the pile, the activation calculation was also effected from the 3D map of the flux when the latter was available, in the same way as for the pile[9]. The impurity levels included are the explanatory impurity levels determined previously by identification in the graphite pile.

The special case of the piles in reactors Chinon A2 and Chinon A3

For the particular case of both Chinon A1 & A2 reactors, for which the samples of graphite were not yet available or used (no measurements available) at the time of writing the present document, it was decided to perform activation calculations using the map of the specific flux obtained by general approximation from the map of Chinon A3 flux, adapted to the particular configurations of Chinon A1 & A2. The impurity levels included are the explanatory impurity levels determined for the graphite pile of Chinon A3 reactor, which was manufactured from cokes of very similar origin.

This decision is motivated by the fact that, as described in the paragraph devoted to the results, it has been observed that the type of graphite, and especially the coke used for its manufacture, is a decisive factor that governs the content and the behaviour of the impurities in the reactor. The pile graphite of the Chinon A3 reactor was manufactured for the most part (74 %) with coke of the Lockport L[10] type, the same type of coke as that used for the Chinon A1 & A2 reactors (see Table 21).

The special case of the sleeves stored in the silos

EDF operates two silos on the site of Saint-Laurent, in which have been stored about 2 000 tonnes of graphite sleeves used in the two Saint-Laurent A1 & A2 reactors. For these sleeves the operational history (neutron flux and length of exposure in the reactor) is very

[9] At the present time only the calculation for the support area of the Bugey 1 reactor had been completed.

[10] The remainder being another variant of Lockport coke (type M), which is very close.

heterogeneous and depends on the operations for renewal of the fuel cartridges during reactor operation. Since the initial cobalt content of the stainless steel retention wires attached to the graphite sleeves varies between 80 and 2 000 mg/kg, variations of dose rate associated with the high presence of cobalt 60 are observed at least in the same proportions. Since the question of radioprotection is particularly important for the retention wires during their storage in the silos, the operator has decided to suspend the automatic but imperfect separation of the retention wire from the graphite of the sleeves. Thus only about a quarter of the retention wires have been separated from the stored graphite sleeves.

The radiological inventory presented in what follows does not take into account these retention wires, and makes no assumptions about the shapes that will be taken by the waste materials during their transportation to the future disposal centre (sleeves intact, in pieces or crushed, and with or without retention wires).

For the sleeves, the process of re-assembling the overall activity is too much complex to be carried out exactly as in the case of a pile, for which both the map of the flux and the unique history are known. The sleeves have undergone different irradiation histories and, for almost 25 % of them, undergone successive irradiation fluxes of different spectra due to re-arrangement of the fuel cartridges in the reactors in operation. In order to perform this re-assembly, various simplifications it is not possible to describe in detail in this report, have been made in order to facilitate the calculations.

The method consists in constructing a typology of the histories of the sleeves into 32 classes. This typology is based on the unloading record chronic of the reactor, which shows that the channels were discharged between 3 to 6 times depending on their irradiation levels. For reasons of symmetry, this typology was established on one-sixth of the core (512 loaded channels or 7 680 fuel positions), which allowed to reconstruct a probable unloading chronic for the 29 712 fuel cartridges. From this typology of the unloading histories of the sleeves, 25 classes of flux were determined.

The methodology for calculation of the inventory by identification calculation–measurement, as described in the previous paragraph, has been applied to these 25 classes of flux by adjustment with the measurements available from the samples of 29 different sleeves whose operational history is known.

5.3.4 The main results

All the results presented relate to an activity calculated for the date of 01/01/2017, this being the initial reference date for withdrawal of the first graphite elements from the Bugey 1 reactor.

Table 19 presents the mass-related activities (in Bq/g) to which is added a 2.5 % risk of under-assessment of the ratio and of the gamma tracer, calculated in the case of the radionuclides of interest covered in this present document. Table 20 presents the calculated inventory (in TBq) for these same radionuclides, with the respective graphite masses expressed in tonnes.

Table 19. Mass activities (in Bq/g) of irradiated graphite from EDF UNGG reactors as determined according to the identification calculation-measurement method

Bq/g	^{3}H	^{10}Be	^{14}C	^{36}Cl	^{41}Ca	^{60}Co	^{63}Ni	^{137}Cs
Chinon A1	$1.1\cdot10^{4}$	13.7	$1.8\cdot10^{4}$	3.4	29.8	$0.2\cdot10^{3}$	$1.3\cdot10^{4}$	19.3
Chinon A2	$2.6\cdot10^{4}$	18.1	$3.9\cdot10^{4}$	6.9	63.8	$0.8\cdot10^{3}$	$2.7\cdot10^{4}$	55.8
Chinon A3	$3.2\cdot10^{4}$	18.6	$4.0\cdot10^{4}$	7.0	65.6	$1.1\cdot10^{3}$	$2.8\cdot10^{4}$	28.7
Snt.-Laur. A1	$2.7\cdot10^{4}$	14.7	$4.0\cdot10^{4}$	2.8	64.1	$0.9\cdot10^{3}$	$2.0\cdot10^{4}$	59.5
Snt.-Laur. A2	$8.9\cdot10^{4}$	19.1	$7.7\cdot10^{4}$	37.9	83.7	$4.0\cdot10^{3}$	$3.5\cdot10^{4}$	47.0
Bugey 1	$9.3\cdot10^{4}$	30.6	$12.6\cdot10^{4}$	82.6	200.0	$7.1\cdot10^{3}$	$7.4\cdot10^{4}$	87.2
Sleeves in silos	$19.9\cdot10^{4}$	17.3	$1.8\cdot10^{4}$	2 620	30.0	$0.4\cdot10^{3}$	$3.5\cdot10^{4}$	294

Table 20. Radiological inventory (in TBq) of irradiated graphite from EDF UNGG reactors as determined according to the identification calculation-measurement method

10^{12} Bq		^{3}H	^{10}Be	^{14}C	^{36}Cl	^{41}Ca	^{60}Co	^{63}Ni	^{137}Cs
Piles	Chinon A1 (1 120 t)	12	0.015	20	0.004	0.03	0.2	14	0.02
	Chinon A2 (2 200 t)	56	0.040	85	0.015	0.14	1.7	60	0.12
	Chinon A3 (2 530 t)	82	0.047	101	0.018	0.17	2.8	72	0.07
	Snt.-Laur. A1 (2 570 t)	70	0.038	102	0.007	0.17	2.2	50	0.15
	Snt.-Laur. A2 (2 440 t)	217	0.047	187	0.092	0.20	9.7	84	0.12
	Bugey 1 (2 060 t)	192	0.063	260	0.170	0.41	14.6	153	0.18
Sleeves in silos (1 990 t)		396	0.03	36	5.21	0.06	0.8	70	0.6
Supports Bugey 1 (525 t)		$2\cdot10^{-2}$	$1\cdot10^{-5}$	$2\cdot10^{-4}$	$5\cdot10^{-6}$	$8\cdot10^{-6}$	$6\cdot10^{-4}$	$3\cdot10^{-3}$	$1\cdot10^{-6}$

The data presented in Table 19 and Table 20 take no account of the influence of leaching phenomena on the graphite of the reactors that are to be dismantled under water (Chinon A3, Saint-Laurent A1 & A2 and Bugey 1). During the dismantling of these reactors, the graphite will be submerged in water for a period of more than 5 years, during which time a certain quantity of radionuclides contained in the graphite will be leached and dissolved in the dismantling water.

Finally, it is recalled that, for the graphite of the sleeves in the silos, the inventory attributed to the retention wires is not included in the presented data.

Exposing the release of some radionuclides in the reactor

The calculation results provide mean values that lead to a distribution of radionuclides subjected to the neutron flux. As illustrated in Fig. 20 in the case of chlorine 36, a greater activity in the central zones of the pile where the neutron flux was the most intense, is logically obtained.

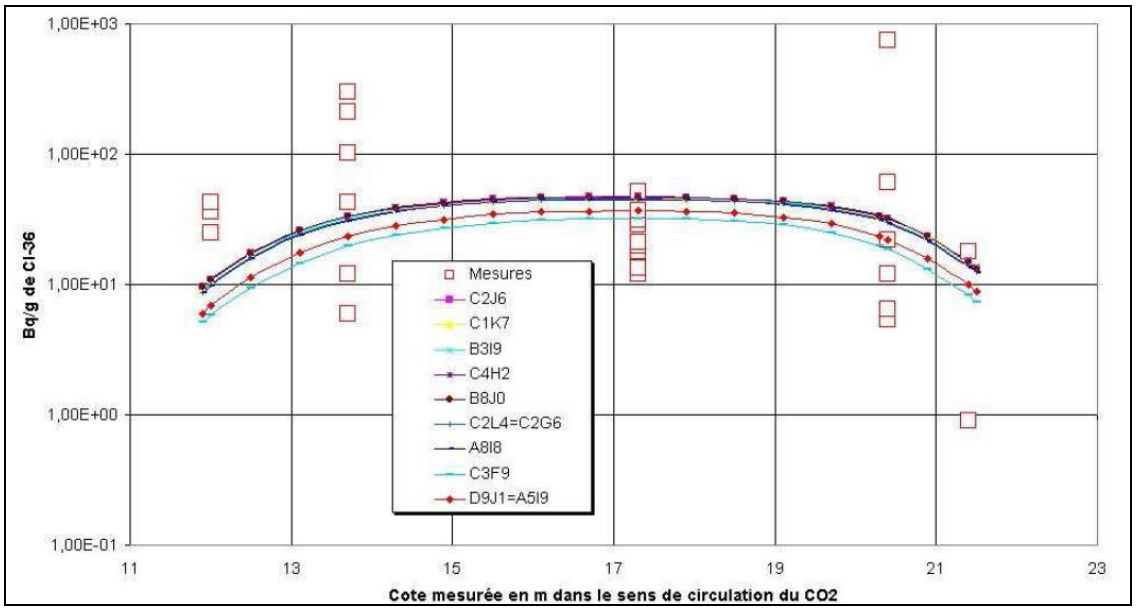

Fig. 20. Average calculated values (in Bq/g) of chlorine 36 for the graphite of some fuel channels in the Bugey 1 graphite pile (squares represent measurements: x-axis – height of the pile)

For the radionuclides that could have been a released by the graphite, adjustment of the value of the explanatory impurity allows us to incorporate this phenomenon. This is the case for chlorine 36, carbon 14 and tritium.

In the case of chlorine 36, it has been shown that the explanatory content of chlorine 36 measured in various samples only corresponds in reality to about 1/100th of the pristine chlorine content in the virgin graphite. The chlorine impurity consistent with the chlorine 36 inventory is of the order of a few hundred of mg/t (wppb) against pristine chlorine content in the non-irradiated graphite of the order of a few tens of mg/kg (wppm).

This result reflects a significant phenomenon of release of the pristine chlorine under the effect of temperature. This phenomenon had indeed been demonstrated and explained in academic studies [46].

In the case of carbon 14, the application of the method also allows to take into account this release phenomenon, probably mainly due to the radiolytic corrosion of the graphite. The carbon 14 calculation results thus show that, in the case of the EDF UNGG reactors, the explanatory nitrogen is much lower than the 50 wppm usually taken as a reference in the literature [36]. For the EDF UNGG reactors, the carbon 14 that remains in the graphite at the end of the operating period originates to a large extent from carbon 13 activation [47].

Absence of meaningful re-deposition of radionuclides on the graphite of the pile

Chlorine release by the pile graphite under operating conditions was observed through measurements performed on the deposits observed at the surface of the metallic internal structures and on the insulating materials inside the reactor vessel (pumice concrete inside reactors Chinon A3, Saint-Laurent A1 & A2). Measurement campaigns performed on similar industrial reactors [44] also highlight the presence of ^{36}Cl in the traps used to dry cooling gas.

This deposition of chlorine 36 observed on the cold parts of the reactor is not measurable for graphite moderator as evidenced by the absence of any spatial correlation of the chlorine 36 measured in the moderator (see Fig. 17). In fact, the regionalised variables resulting from pollution or deposition would present a continuum characterised by a random irregularity which would always lead us to consider a spatial interpolation. In the vocabulary of “geostatistics”, the non-applicability of such an assumption to the available measurements corresponds to a pure “nugget effect” (we also say 100 % “nugget effect”). By definition, this effect is the negation of a significant deposit since it corresponds to the lack of any correlation between the measured values (for example chlorine 36 activity) at two points were they should be very close.

The final argument of this pure nugget effect lies in the fact that a significant percentage of crushed graphite samples with a press of a few tonnes in another laboratory of the CEA, instead of the 150 tonnes as described above, resulted in measurements on samples which are not consistent in pairs. Indeed, their measurement uncertainty intervals (to 2 σ) are disjointed when it concerns two test specimens from the same crushed core batch. This means that the non-correlation of nearby points is so strong in the original graphite (100 % nugget effect) that even a crushing session followed by a careful mixing is not able to lower this non-correlation to the point where it remains detectable.

This comment on the absence of any significant deposit of radionuclides on the graphite from the pile is nothing inconsistent with what has been described at hydrogen-carbonated deposits observed in the reactors, where low methane content was added in the cooling gas [48]. In fact in this case, it is a simple deposit resulting from a chemical phenomenon analogous to polymerisation which was produced under the effect of temperature and of the radiation within the operating reactor. That phenomenon is without any significant effect on the inventory of the radionuclides measured in the waste (especially chlorine 36).

Graphite behaviour as a function of the origin of the coke

Another very interesting result for chlorine 36 concerns the influence of the different graphite used in the reactors. Depending on the coke used for the manufacture of the different graphite, inventories of different magnitudes were observed. Thus the radiological inventory is higher in the graphite that was produced from Lima coke (Saint-Laurent A2 and Bugey 1). This result is particularly striking when the results obtained on the Saint-Laurent A1 & A2 reactors whose designs and operating conditions are identical, are compared. For Saint-Laurent A1, whose pile is made of graphite produced from Lockport M coke, the radiological inventory is significantly lower in chlorine 36 (about one order of magnitude less), than in Saint-Laurent A2 whose pile is made of graphite produced from Lima coke (see Table 21).

This result may be due to impurities depending on the coke used for graphite manufacture, or to the graphite behaviour concerning the radionuclides release. These two reasons are not necessarily mutually exclusive but the same chlorine behaviour for Saint-Laurent A2 and Bugey 1 piles shows that the coke effect is preponderant because these two reactors have clearly different operating conditions but the same Lima coke. The experimental results from

previous work tend to show that the release seems to be lower in the case of the graphite produced from Lima coke than for those produced from Lockport.

The rediscovery of the influence of the coke used for the graphite manufacture is a particularly noteworthy result of the method developed for the assessment of the graphite inventory. This information has indeed not been taken into account in the development of the method. No preliminary favour arbitrary assumption was done. This observation relies only on the radionuclide measurements and on the use of the method. The influence of the coke parameter is a given tangible, simple and natural result of the calculation method which confirms its relevance and effectiveness.

Table 21. Mean chlorine 36 mass activity calculated by the identification calculation-measurement method for different type of graphite in UNGG reactors

UNGG reactor	Graphite mass pile (t)	Specific power (W_{th}/g U)	Coke used for graphite manufacturing	Mean ^{36}Cl mass activity (Bq/g)
Chinon A1	1 120	2.1	Lockport L	1.0
Chinon A2	2 200	3.1	Lockport L	2.1
Chinon A3	2 530	3.2	Lockport L (74 %) Lockport M (26 %)	2.1
Snt.-Laur. A1	2 570	3.7	Lockport M	1.7
Snt.-Laur. A2	2 440	3.8	Lima	18.2
Bugey 1	2 060	5.7	Lima	25.5

The particular case of fission products

The results for caesium 137 (tracer element of the fission reactions) shows that decontamination actions adopted after the two accidents involving the melting of some fuel cartridges in Saint-Laurent A1 & A2 reactors were effective. These accidents have indeed no detectable effect in terms of contamination of the graphite. Levels of caesium 137 are substantially equivalent in all EDF reactors, whether melting of fuel elements has occurred (Saint-Laurent reactors), or not. The presence of caesium 137 in very small quantities and the heavy nuclei produced are also explained by the fission of traces of uranium present in the graphite. These traces were identified through the chemical analysis performed on the graphite at the time of manufacturing and discovered by the method for inventory calculation by identification calculation-measurement.

5.4 Conclusions

The use of the new method for the inventory calculation proposed by EDF can be achieved when corresponding measurements of radionuclides are available. It allows obtaining a preliminary assessment of the impurity at the origin of these radionuclides instead of postulated values. This was possible thanks to the acquisition of new samples measurements since the establishment of the MIP 2007 ANDRA. This method contributes to calculate a more accurate radiological inventory related to the physical phenomenon at the origin of radionuclides. The main benefit of applying this method to the irradiated graphite from EDF reactors regards the inventory of the radionuclides present at the trace level. For these radionuclides such as chlorine 36, an approach based only on a few measurements of maximum activity such as chosen in the development of the MIP 2007, lead to an extremely conservative assessment that is unrealistic and moreover very penalizing for the future waste management.

The benefit of this method is particularly marked in the case of chlorine 36 whose very low content implies a large observed variability of the measurements. It is essential in that particular case, to use a representative panel (in sufficient number) of measurements to establish a realistic inventory. For the irradiated graphite of the EDF reactors, compared to the MIP 2007, the chlorine 36 inventory passes from 21.4 TBq (including 8.5 TBq for the sleeves of the Saint-Laurent silos) to 5.5 TBq (including 5.2 TBq only for these sleeves).

It is in the graphite of the sleeves of the Saint-Laurent silos where the main part of the chlorine 36 activity of EDF graphite waste is located. The 2 000 tonnes of graphite sleeves of the Saint-Laurent silos contain approximately 5.2 TBq chlorine 36 against about 0.3 TBq for the 13 000 tonnes of irradiated graphite from the piles. In cases where the chlorine 36 would be a particular difficulty for the future management of waste graphite, then separate management of the graphite of the silos from that of the graphite from the piles could logically be considered.

It may be noted by comparing inventories presented in Table 20, the graphite of Bugey 1 core presents the highest radiological activities, except for the sleeves stored in the Saint-Laurent silos. It is in this reactor that the highest neutron flux densities have been reached.

Finally, the graphite of the biological shield located in the support area of integrated reactors (Bugey 1, Saint-Laurent A1 & A2) is logically much less active (zone of very low neutron

flux). It will be noted that this graphite, which represents a total mass of the order of 2 000 tonnes, is currently classified in the category of LLW-LL (low level activity waste / long-lived: FA-VL in French), while their long-lived radionuclide content is well below the Maximum Activity Limit (LMA) in long-lived radionuclides acceptable in the ILW (Intermediate Level Waste) category currently stored in the ANDRA ILW surface repository centre (CSFMA in French). For example, the graphite of the support area of the Bugey 1 reactor contains on average only $8.55 \cdot 10^{-3}$ Bq/g of chlorine 36 which is 585 times less than the current LMA of the CSFMA.

6 References

6.1 References of chapter 2

1. *Almenas, K.; Kaliatka, A.; Uspuras, E.* Ignalina RBMK-1500: A Source Book. 2nd ed. Kaunas: Lithuanian Energy Institute, 1998. 196 p.
2. Characterization, Treatment and Conditioning of Radioactive Graphite from Decommissioning of Nuclear Reactors: IAEA TECDOC No. 1521. Vienna: International Atomic Energy Agency, 2006. 71 p.
3. Graphite Decommissioning: Options for Graphite Treatment, Recycling, or Disposal, Including a Discussion of Safety-Related Issues. EPRI, Palo Alto, CA: 2006. 1013091.
4. Assessment of Isotope-accumulation Data from RBMK-1500 Reactor. Technical Report T-3.4.2, CARBOWASTE Project.
5. *Ancius, D.; et al.* Evaluation of the Activity of Irradiated Graphite in the Ignalina Nuclear Power Plant RBMK-1500 Reactor. Nukleonika, 2005, vol. 50, no. 3, p. 113−120.
6. *Bylkin, B. K.; et al.* Induced Radioactivity and Waste Classification of Reactor Zone Components of the Chernobyl Nuclear Power Plant Unit 1 after Final Shutdown. Nuclear Technology, 2001, vol. 136, p. 76–88.
7. *Bushuev, A. V.; Zubarev, V. N.; Proshin, I. M.* Impurity Composition and Content in Graphite from Commercial Reactors. Atomic Energy, 2002, vol. 92, no. 4, p. 331–335.
8. *Smaizys, A.; Narkunas, E.; Poskas, P.* Modelling of Activation Processes for GR-280 Graphite at Ignalina NPP. Radiation Protection Dosimetry, 2005, vol. 116, no. 1–4, p. 270–275.
9. *Davis, W. Jr.* Carbon-14 Production in Nuclear Reactors, NRC Report, ORNL/NUREG/TM-12, Oak Ridge National Laboratory, NTIS, February 1977.
10. *Khripunov, V. I.; Kurbatov, D. K.; Subbotin, M. L.* C-14 Production in CTR Materials and Blankets. Proceedings of 21st Fusion Energy Conference (FEC 2006), p. 16–21 October 2006. Chengdu, China. SE/P2-3.
11. Ignalina NPP Safety analysis Report. Ignalina, 1996.

12. Safety Analysis Report for INPP Unit 2. Ignalina, 2003.
13. *Hacker, P. J.; Neighbour, G. B.; Levinskas, R.; Milcius, D.* Characterization of Ignalina NPP RBMK Reactors Graphite. Materials Science, 2001, no. 1, p. 62–66.
14. *Bondarkov, M. D.; et al.* Activity Study of Graphite from the Chernobyl NPP Reactor. Bulletin of the Russian Academy of Science: Physics, 2009, no. 2, p. 261–265.
15. *Poncet, B. R.* Characterization of Graphite Sleeves from Bugey 1 EDF Plant for Permanent Disposal – Measurement and Calculation of Scaling Factors for Difficult-to-Measure Nuclides. WM'03 Conference, February 2003, Tucson, Arizona, USA.
16. First Radionuclide Inventory Data on Untreated Graphite / Evaluation for Direct Disposal. Deliverable D-3.3.1, CARBOWASTE Project.

6.2 References of chapter 3

17. Assessment of Isotope-accumulation Data from MTR. Technical Report T-3.4.1, CARBOWASTE Project.

6.3 References of chapter 4

18. NDA Report. Radioactive Wastes in the UK: A Summary of the 2001 Inventory. Report No. DEFRA/RAS/02/003, NIREX Report N/041, 2002.
19. NDA Report. Final Waste Issues Group Report, 2007.
20. NDA Report. Radioactive Wastes in the UK: A Summary of the 2010 Inventory, 2010.
21. *Banford, A.; Eccles, H.; Graves, M.; von Lensa, W.; Norris, S.* CARBOWASTE – An Integrated Approach to Irradiated Graphite. Nuclear Futures, 2008.
22. Activation Modelling of Graphite to Advise Retrieval Solutions. Deliverable D-2.3.1D, CARBOWASTE Project.
23. Characterization, Treatment and Conditioning of Radioactive Graphite from Decommissioning of Nuclear Reactors: IAEA TECDOC No. 1521. Vienna: International Atomic Energy Agency, 2006. 71 p.
24. *Nightingale, R. E.* Nuclear Graphite. Academic Press, New York and London, 1962.

25. *Gerlach, D. C.; Cliff, J. B.; Hurley, D. E.; Reid, B. D.; Little, W. W.; Meriwether, G. H.; Wickham, A. J.; Simmons, T. A.* Secondary ionization mass spectrometric analysis of impurity element isotope ratios in nuclear reactor materials. Applied Surface Science, 252, 2006, p. 7041–7044.
26. *Takahashi, R.; Toyahara, M.; Maruki, S.; Ueda, H.; Yamamoto, T.* Investigation of Morphology and Impurity of Nuclear Grade Graphite, and Leaching Mechanism of Carbon-14. Nuclear Graphite Waste Management: Proceedings of Technical Committee Meeting, October 18–20, 1999, Manchester, United Kingdom. Vienna: International Atomic Energy Agency, 2001, p. 176–190.
27. *White, I. F.; Smith, G. M.; Sauders, L. J.; Kaye, C. J.* Assessment of Graphite Management Modes for Graphite from Reactor Decommissioning, 1984.
28. The ANSWERS Software Service, WIMS9 User Guide, ANSWERS/WIMS(99)9.
29. *Forrest, R. A.* FISPACT-2007: User Manual. Report UKAEA FUS 534, 2007.
30. *Marsden, B. J.; Wickham, A. J.* Graphite disposal options – A comparison of the approaches proposed by UK and Russian reactor operators. Proc. of International Conference on Nuclear Decommissioning '98, IMechE, 1998, p. 145–153.
31. *Von Lensa, W.; et al.* CARBOWASTE: New EURATOM Project on "Treatment and Disposal of Irradiated Graphite and other Carbonaceous Waste". Proceedings of the 4th International Topical Meeting on High-temperature Reactor Technology (HTR2008). Washington D.C. USA, 2008.

6.4 References of chapter 5

32. Production of Summary Report of the Various Options Identifying Key Issues. Summary Report on Work Package No. 1. Deliverable D-1.1.4, CARBOWASTE Project.
33. Radiological Characterization of Shut Down Nuclear Reactors for Decommissioning Purposes: IAEA TECDOC No. 389. Vienna: International Atomic Energy Agency, 1998. 184 p.
34. Website: http://www.nndc.bnl.gov/chart/chartNuc.jsp

35. Website: http://www.ncnr.nist.gov/resources/n-lengths/list.html
36. *Marsden B. J.; Hopkinson K. L.; Wickham A. J.* The Chemical Form of C-14 within Graphite. Serco Assurance Technical Report for NIREX: SA/RJCB/RD03612001/R01, 2002.
37. *Bonal J. P.; Bresard I.; Parraud S.* Caractérisation du graphite des réacteurs de la filière UNGG. Matériaux 1-5, 2002.
38. *Braun H.; Gutowski H.; Bonka H.; Grundler D.* Plant for Retention of ^{14}C in Reprocessing Plants for LWR Fuel Elements. Proceedings of 17th DOE Nuclear Air Cleaning Conference 1983, CONF-820833:381-399.
39. *Clayton A. M.; Harper A.; Wheatley C. J.* Behaviour of Chlorine in Nuclear Graphite. AEA Technology Technical Report for NIREX: T/REP/20121/P/04, 1997.
40. Website: http://www.protem.fr
41. First Radionuclide Inventory Data on Untreated Graphite / Evaluation for Direct Disposal. Deliverable D-3.3.1, CARBOWASTE Project.
42. *Gy P.* Sampling of heterogeneous and dynamic material systems, theories of heterogeneity, sampling and homogenizing. Elsevier, 1992, Amsterdam, 653 p.
43. *Takahashi R.; Toyahara, M.; Maruki, S.; Ueda, H.; Yamamoto, T.* Investigation of Morphology and Impurity of Nuclear Grade Graphite, and Leaching Mechanism of Carbon-14. Nuclear Graphite Waste Management: Proceedings of Technical Committee Meeting, October 18–20, 1999, Manchester, United Kingdom. Vienna: International Atomic Energy Agency, 2001, p. 176–190.
44. *Brown F. J.; Palmer J. D.; Wood P.* Derivation of a Radionuclide Inventory for Irradiated Graphite – Chlorine-36 Inventory Determination. Nuclear Graphite Waste Management: Proceedings of Technical Committee Meeting, October 18–20, 1999, Manchester, United Kingdom. Vienna: International Atomic Energy Agency, 2001, p. 143–152.
45. *Poncet B.* EDF Radioactive Inventories Based on Hundreds of Measurements Are Casting Doubt on 'a Priori' Accepted Ideas. WM'10 Conference, March 2010, Phoenix, Arizona, USA.

46. *Vaudey C. E.* Study of the Effects of Temperature and Radiolysis on Chlorine Distribution in Nuclear Graphite. PhD Thesis of the University Claude Bernard Lyon 1, 2010 (in French).
47. *Poncet B.; Petit L.* EDF Analysis on the Origins of Carbon 14 in UNGG Cores. 8th EPRI International Decommissioning and Radioactive Waste Workshop: CARBOWASTE SESSION Held on 7 October 2009 in Hamburg, Germany.
48. *Petit A.; Brie M.* Graphite Stack Corrosion of Bugey 1 Reactor (Synthesis). Graphite Moderator Lifecycle Behaviour: Proceedings of a Specialists Meeting, September 24–27, 1995, Bath, United Kingdom. Vienna: International Atomic Energy Agency, 1995, p. 167–180.